Spin Structure with Polarized ^{3}He

- A few physics highlights using polarized ^{3}He
  - the target improvements that enabled the experiments
- Upcoming experiments using polarized ^{3}He
  - the target improvements that WILL enable the experiments
- Target considerations specific to spectator-tagging experiments

Gordon Cates,
HE NP w Spectator Tagging 2015
Old Dominion
March. 9, 2015

University of Virginia

Spin physics using polarized ^3He

The spin structure of the neutron at SLAC: E142 and E154 - used the first liter-sized polarized ^{3}He targets

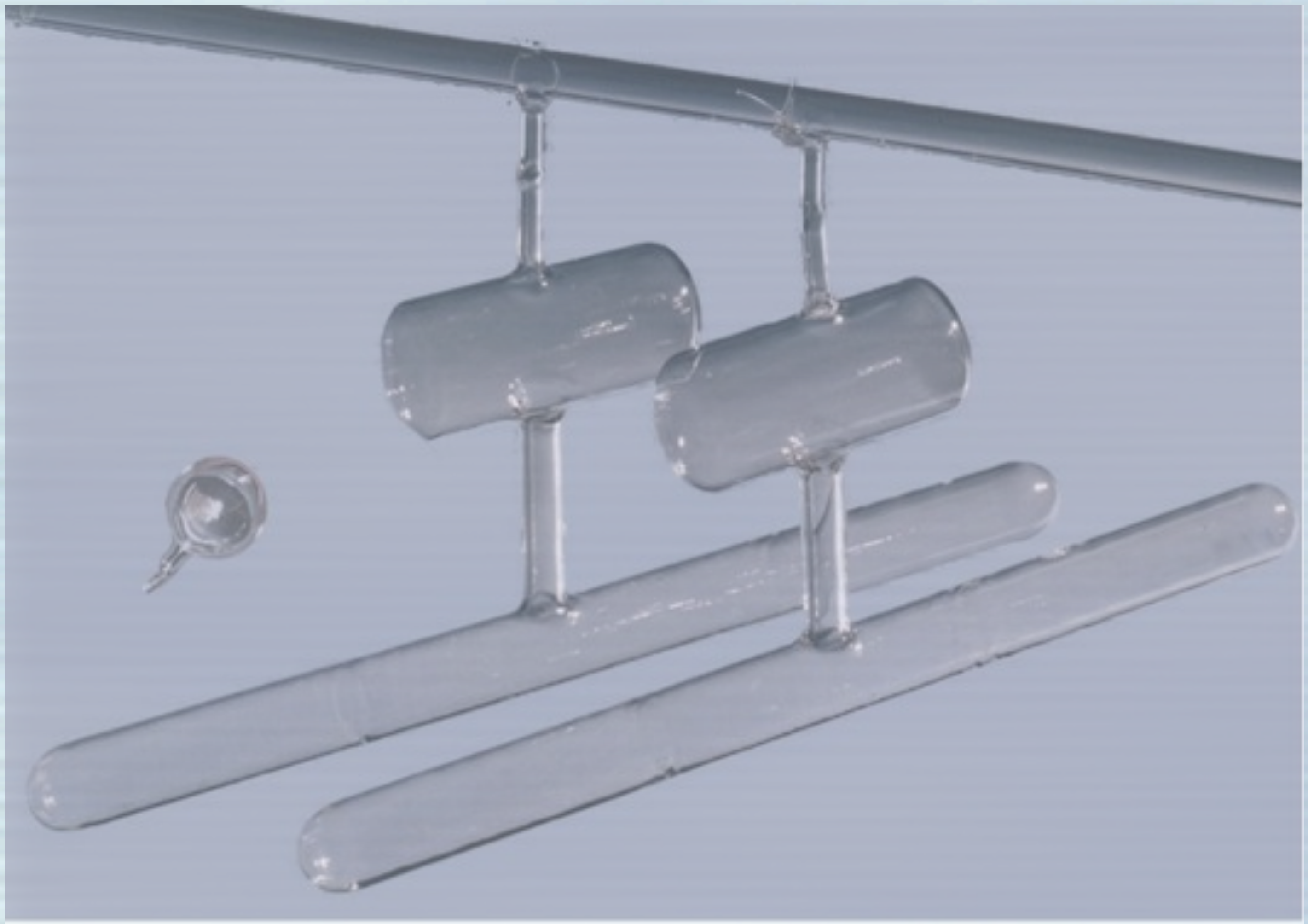

With volumes of 150-200 cc's and nearly 10 atmospheres, these targets contained 1-2 STP liters of gas.

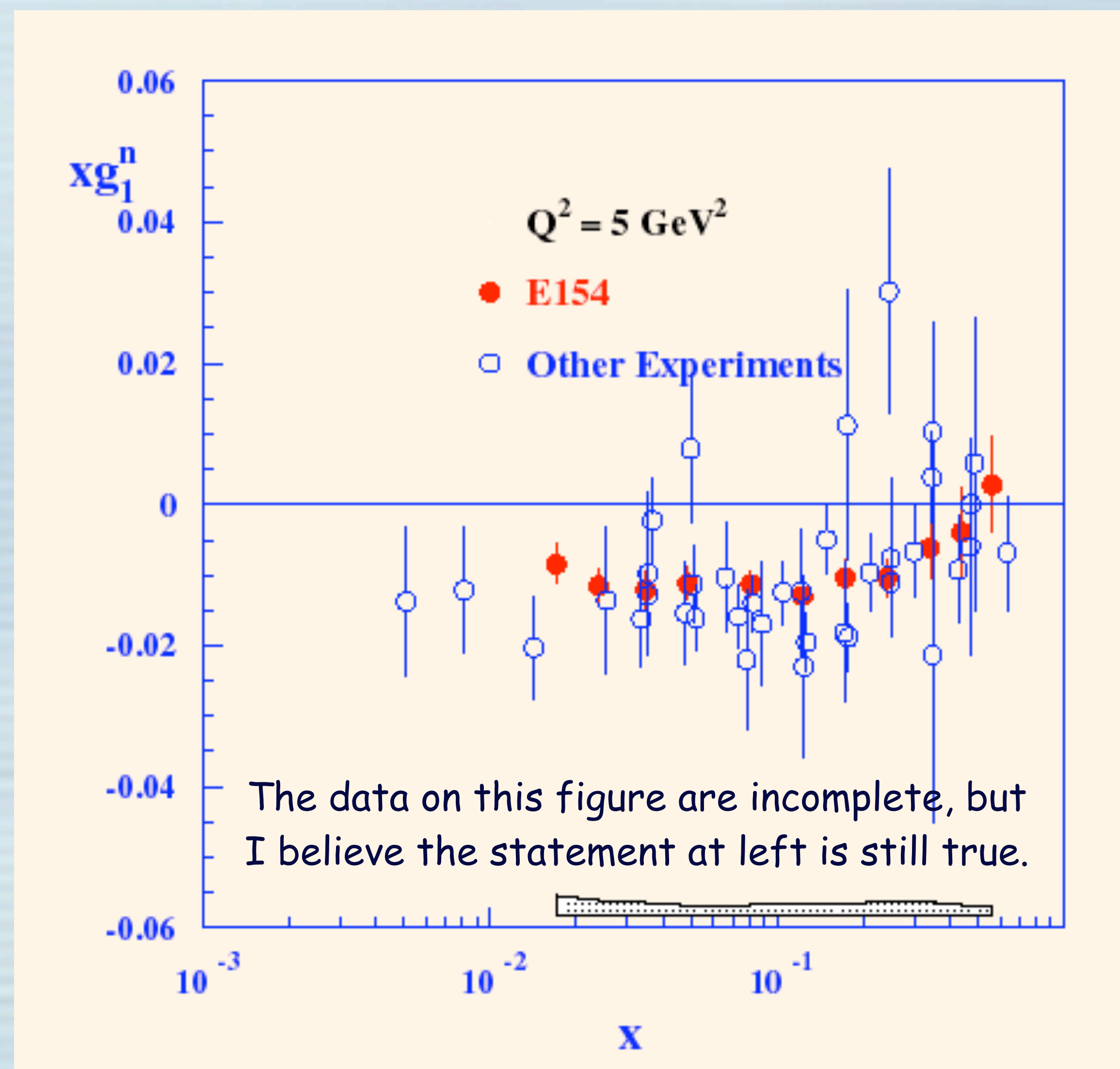

To this day, the data from E142 and E154 provide the most accurate data on the spin structure functions of the neutron over the kinematic range studied.

Q^2 Evolution of the Generalized Gerasimov-Drell-Hearn Integral for the Neutron using a ^3He Target

- Connected well understood behavior in the regimes dominated by hadronic degrees of freedom and partonic degrees of freedom.
- Provided test of extending GDH Sum Rule using Chiral Perturbation theory.
- First use of polarized ^3He target at JLab.
- Provided a critical piece for determining the Q2 evolution of the Bj Sum Rule

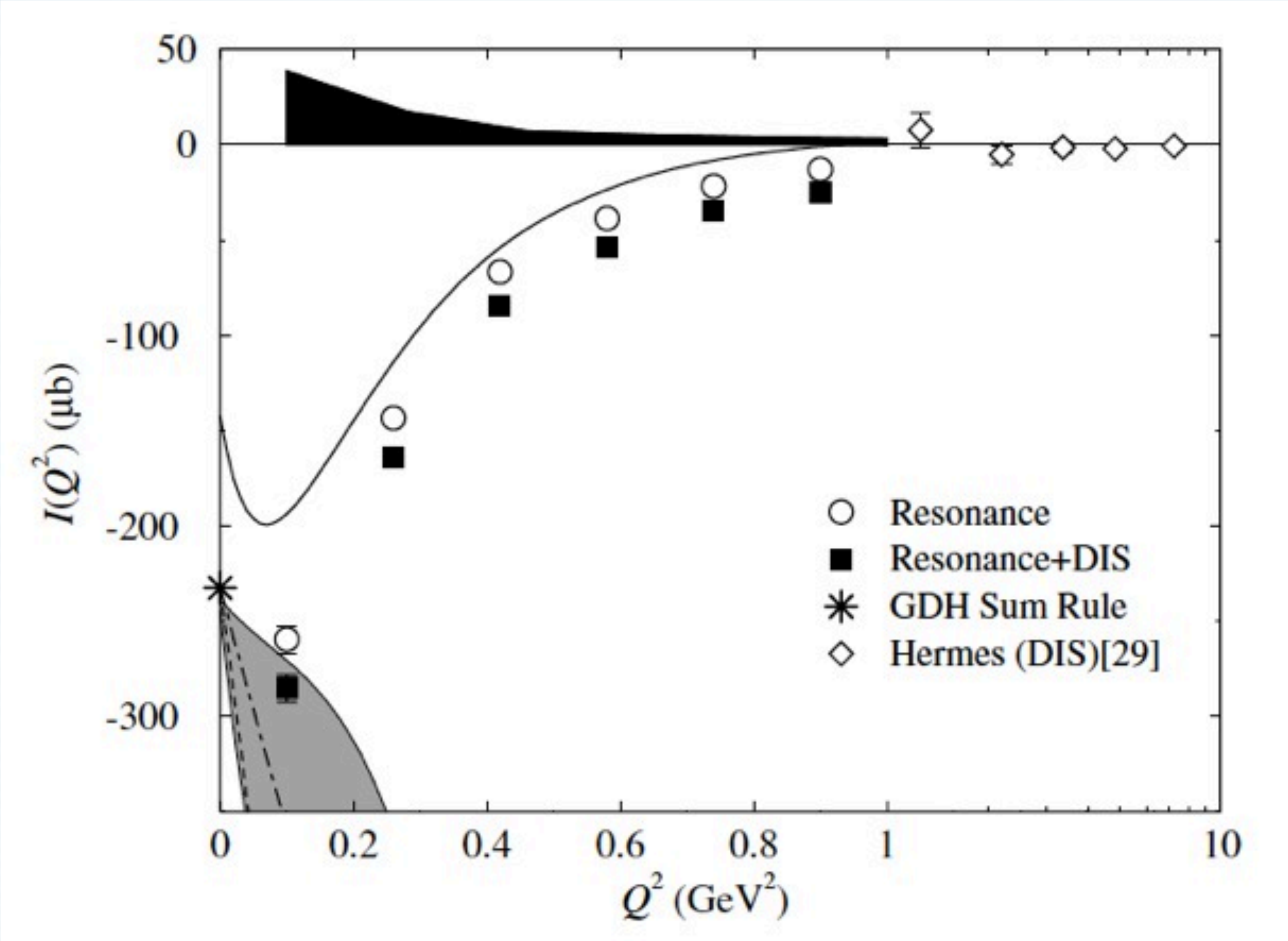

M. Amarian et al., PRL vol. 89, pg 242301 (2002)

Experimental Determination of the Evolution of the Bjorken Integral at Low Q^2

- Combined ^{3}He, D and proton data.
- Provides unique connection between hadronic and partonic regimes.
- Used by Bill Marciano to constrain hadronic box diagrams in his analysis of the unitarity of the CKM matrix
- Thus played a (little) role in the 2008 Nobel Prize to Nambu, Kobayashi and Maskawa

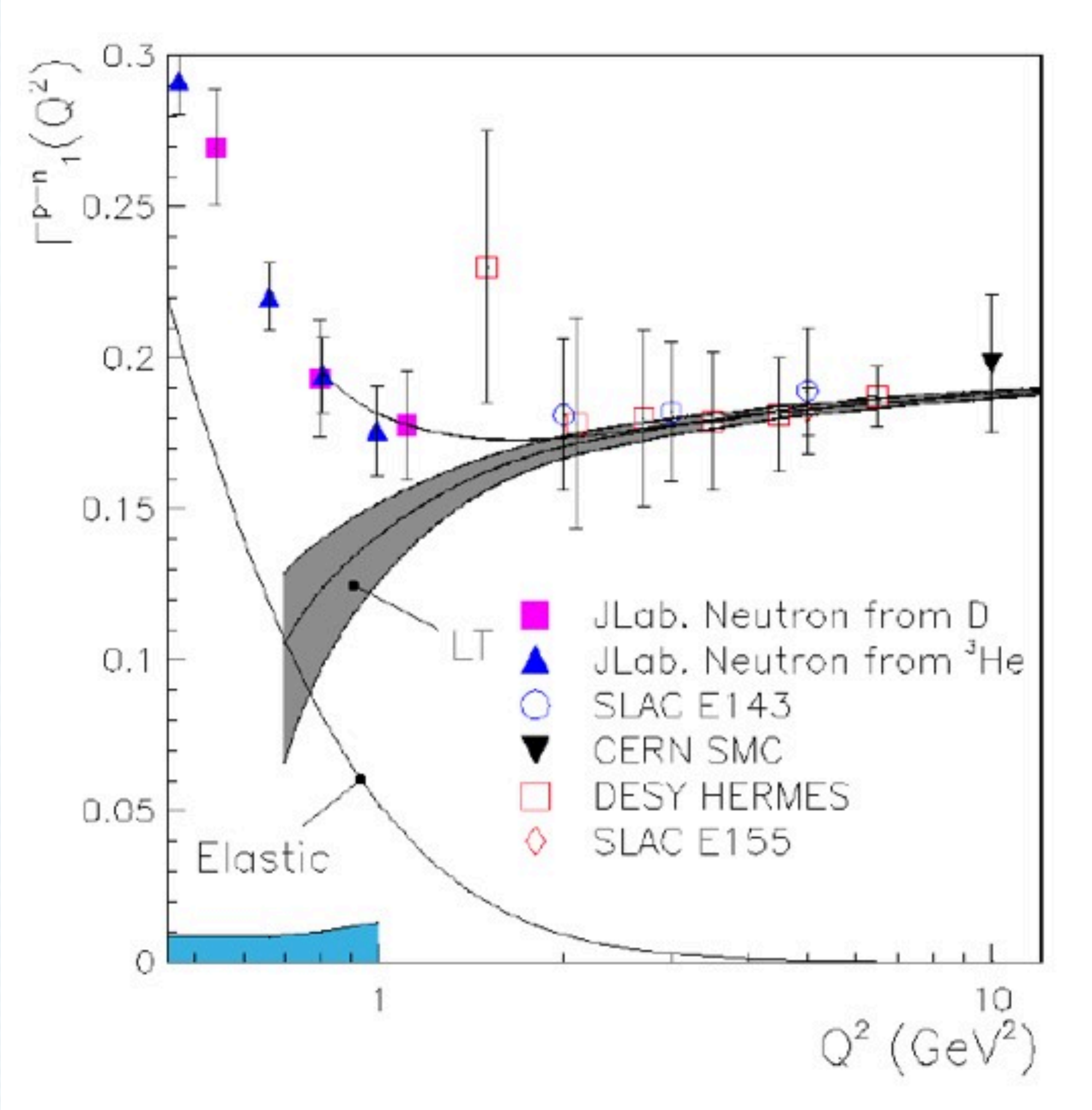

A. Deur et al., PRL vol. 93, pg 212001 (2004)

The spin asymmetry A_1^n in virtual photoabsorption cross section of the neutron

- Pushed A1n measurement up to x = 0.6.
- First observation of A_1^n becoming positive.
- Clearly more consistent with RCQMs than with assumption of hadron helicity conservation.
- Early confirmation of the importance of quark OAM following the observation of the Q^2 dependence of G_E^p/G_M^p

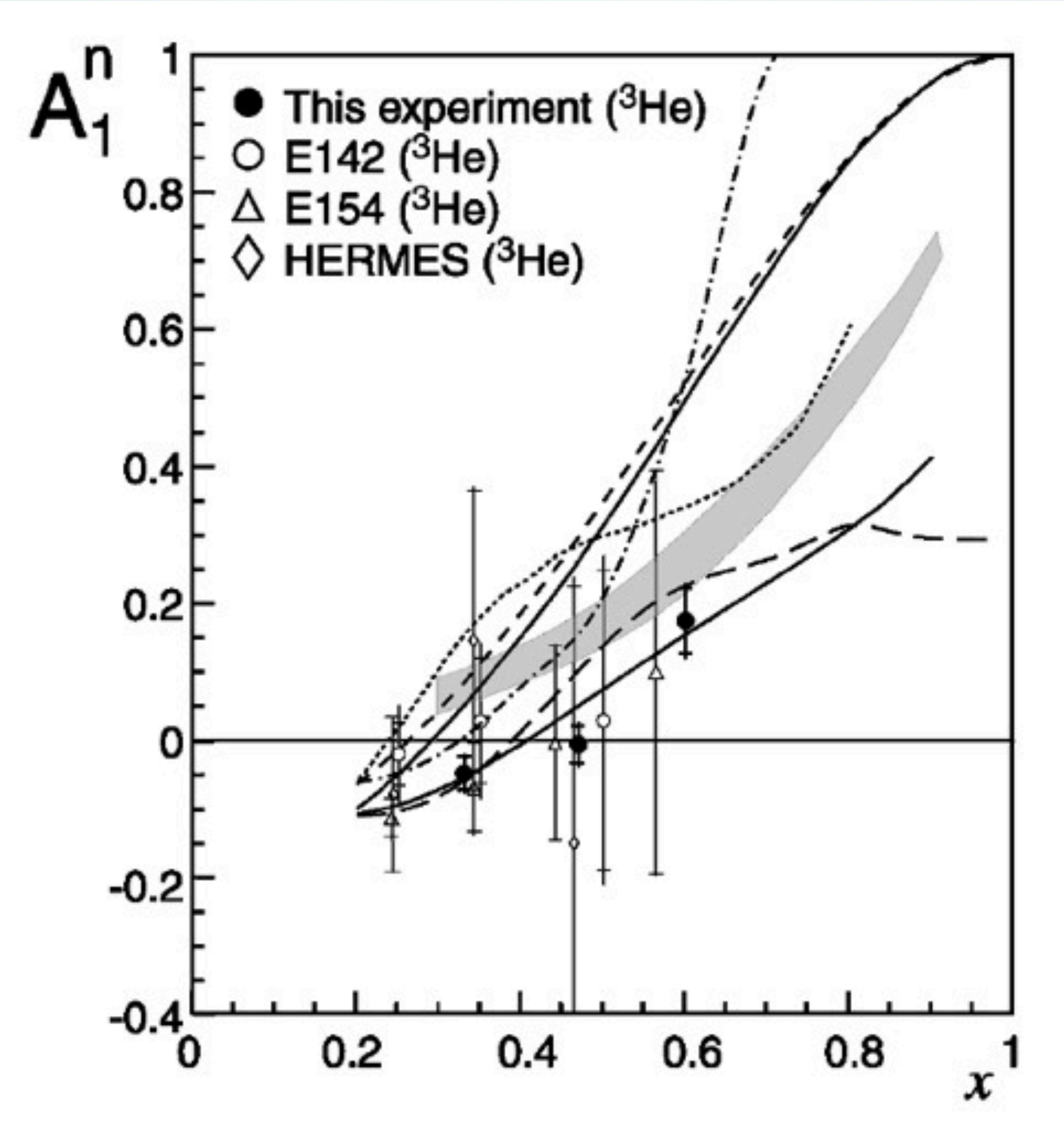

Zheng et al., PRL vol. 92, pg 012004 (2004)

The Electric Form Factor of the Neutron at high Q^2

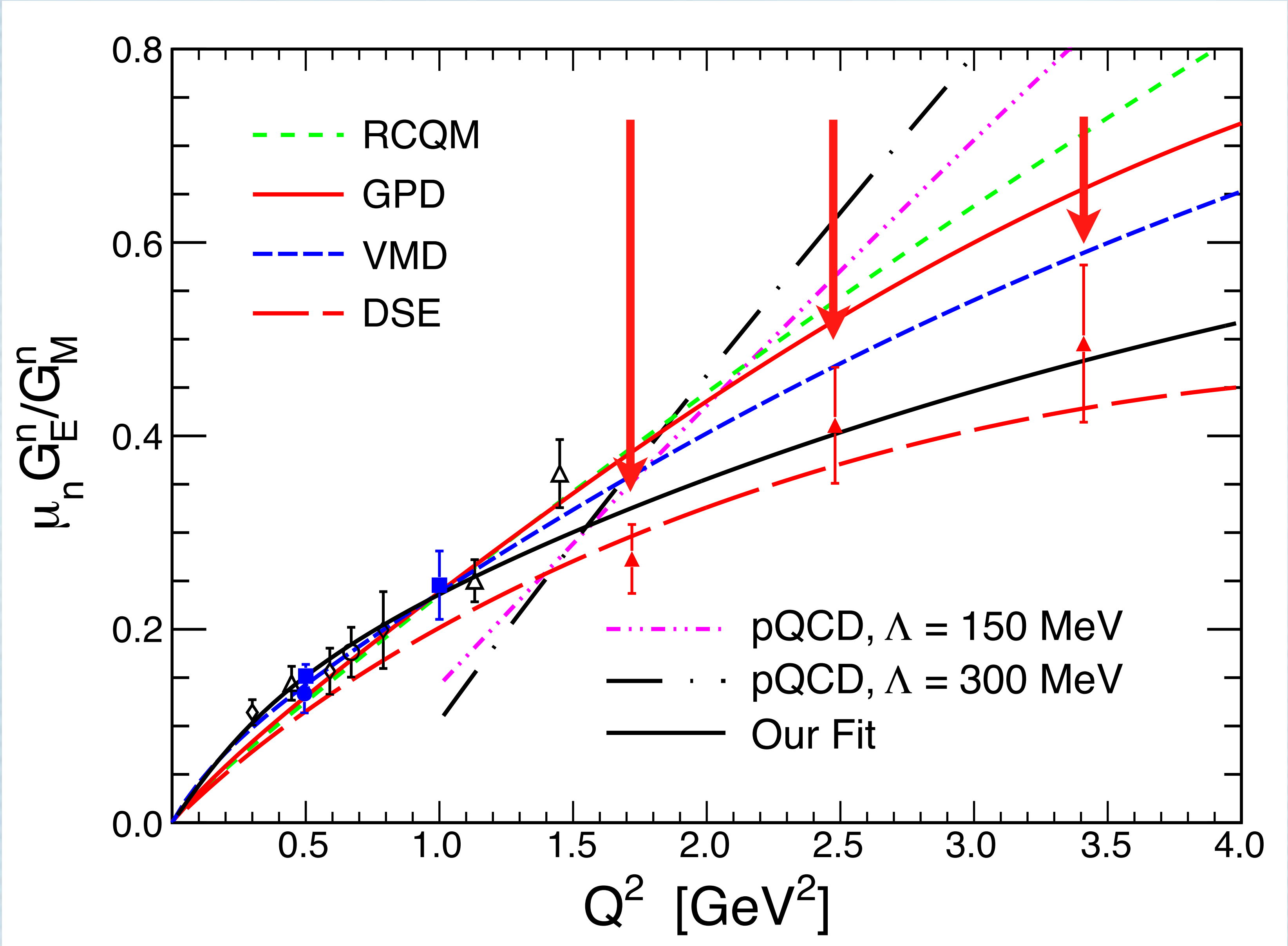

Riordan et al., PRL vol. 105, pg 262302 (2010)

- Matched the Q^2 range of the first JLab measurement of G_E^p/G_M^p
- Generally supported new theoretical treatments of proton structure that were triggered by the measurement of G_E^p/G_M^p
- Made it possible to perform a flavor separation of the elastic nucleon FFs.

Flavor-separated elastic form factors

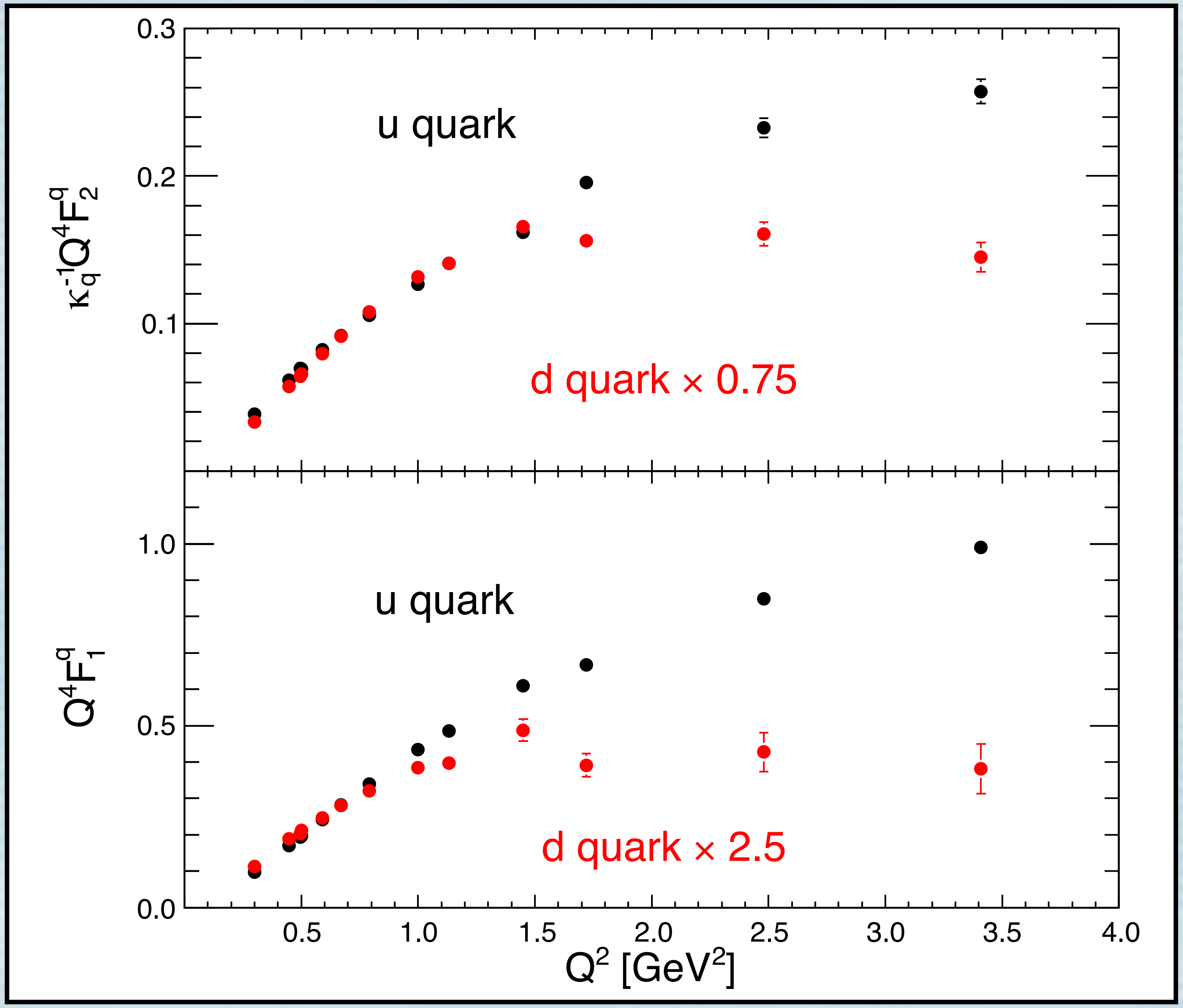

Cates, de Jager, Riordan and Wojtsekhowski, PRL vol. 106, pg 252003 (2010)

Different Q^2 ^{be}libehavior has been interpreted as evidence supporting the importance of diquark degrees of freedom

Single Spin Asymmetries in Charged Pion Production from Semi-Inclusive Deep Inelastic scattering on Transversely Polarized ^{3}He target at Q^2 = 1.4 - 2.7 GeV^2

Qian et al., PRL vol. 107, pg 072003 (2011)

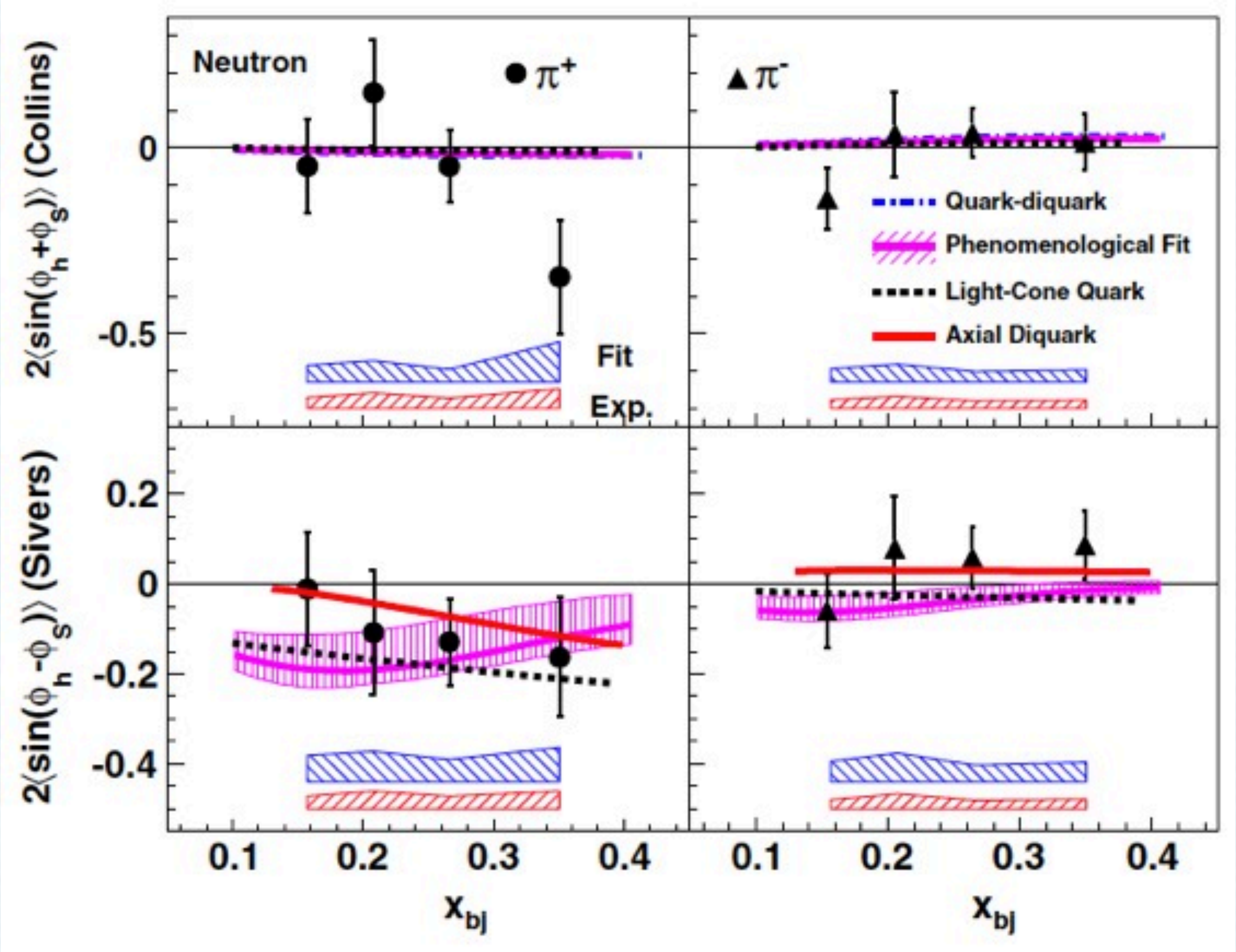

- Limited statistical power, but important demonstration of the feasibility of SSA studies in SIDIS using polarized ^{3}He.
- Non-zero Sivers moment can be viewed as smoking gun for quark OAM

Spin-exchange optical pumping

Two-step process:

1. alkali vapor is optically pumped.

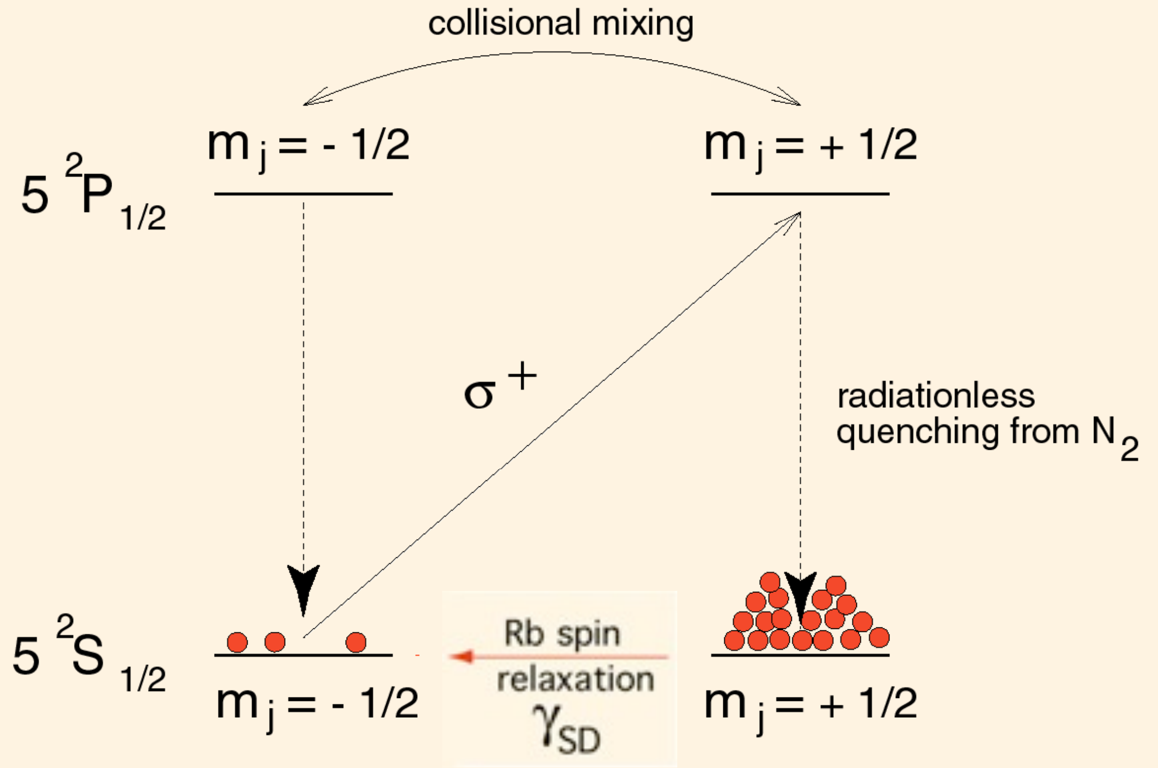

2. noble-gas nuclei are polarized through spin- exchange collisions

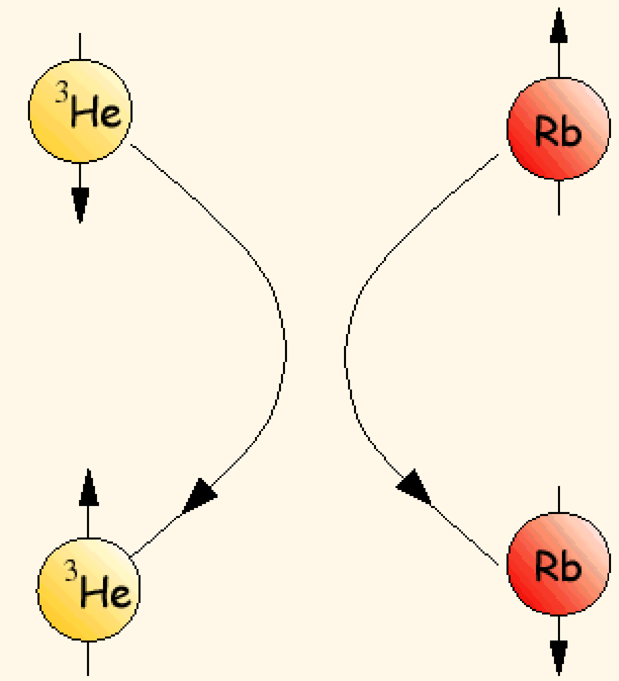

For ^{129}Xe, spin exchange in van der Waals molecules formed in three-body collisions also plays an important role.

Important technology

- High-power diode-laser arrays (SLAC E154/JLab E-94-010 (GDH))
- Careful selection through full-power tests (E-99-117 (A1n))
- Alkali-hybrid spin-exchange optical pumping (GEn)
- Spectrally-narrowed high-power diode-laser arrays (Transversity)

The performance of polarized ^{3}He targets have increased by roughly a factor of 30 since SLAC E142

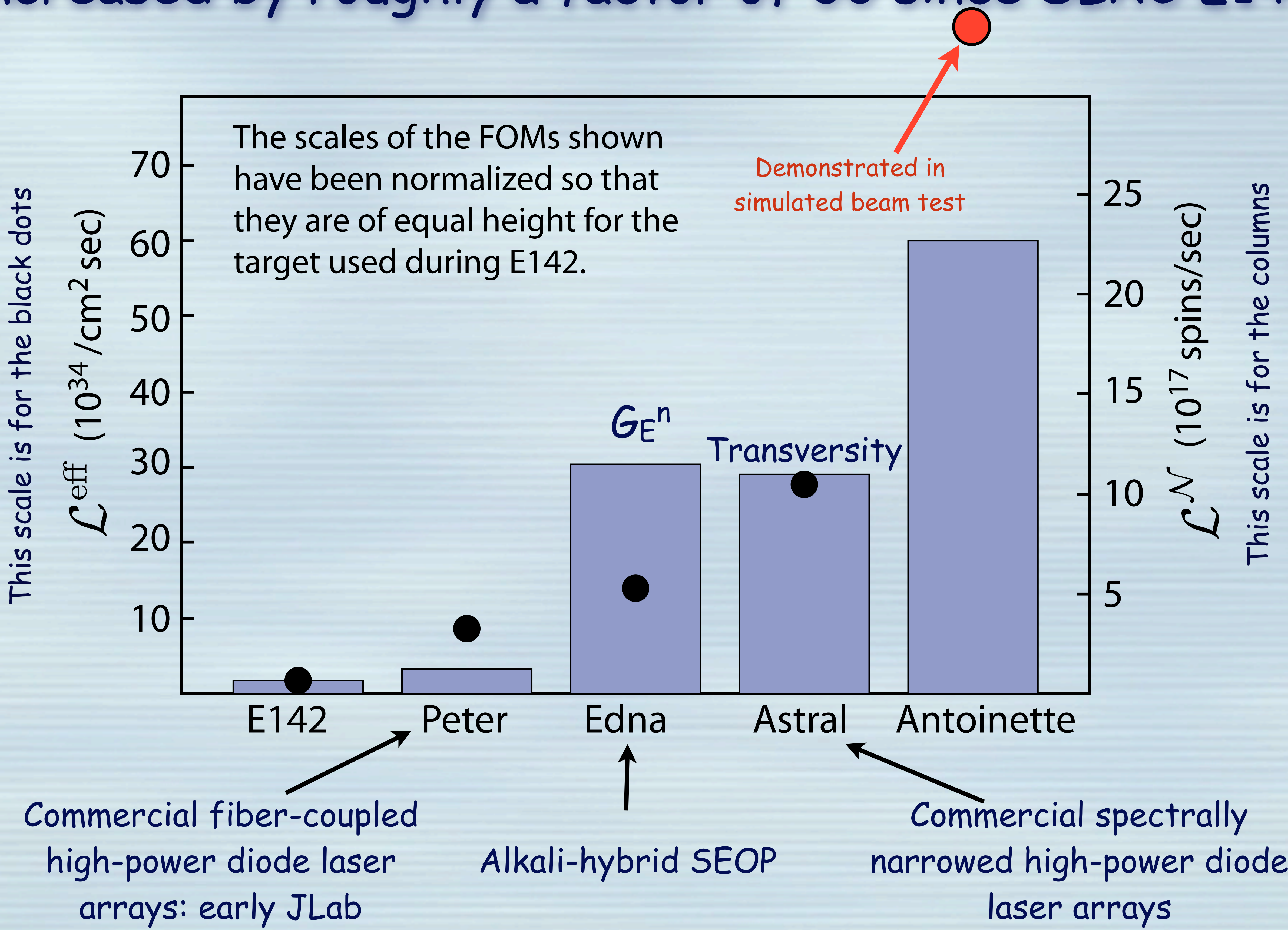

Most recent JLab targets

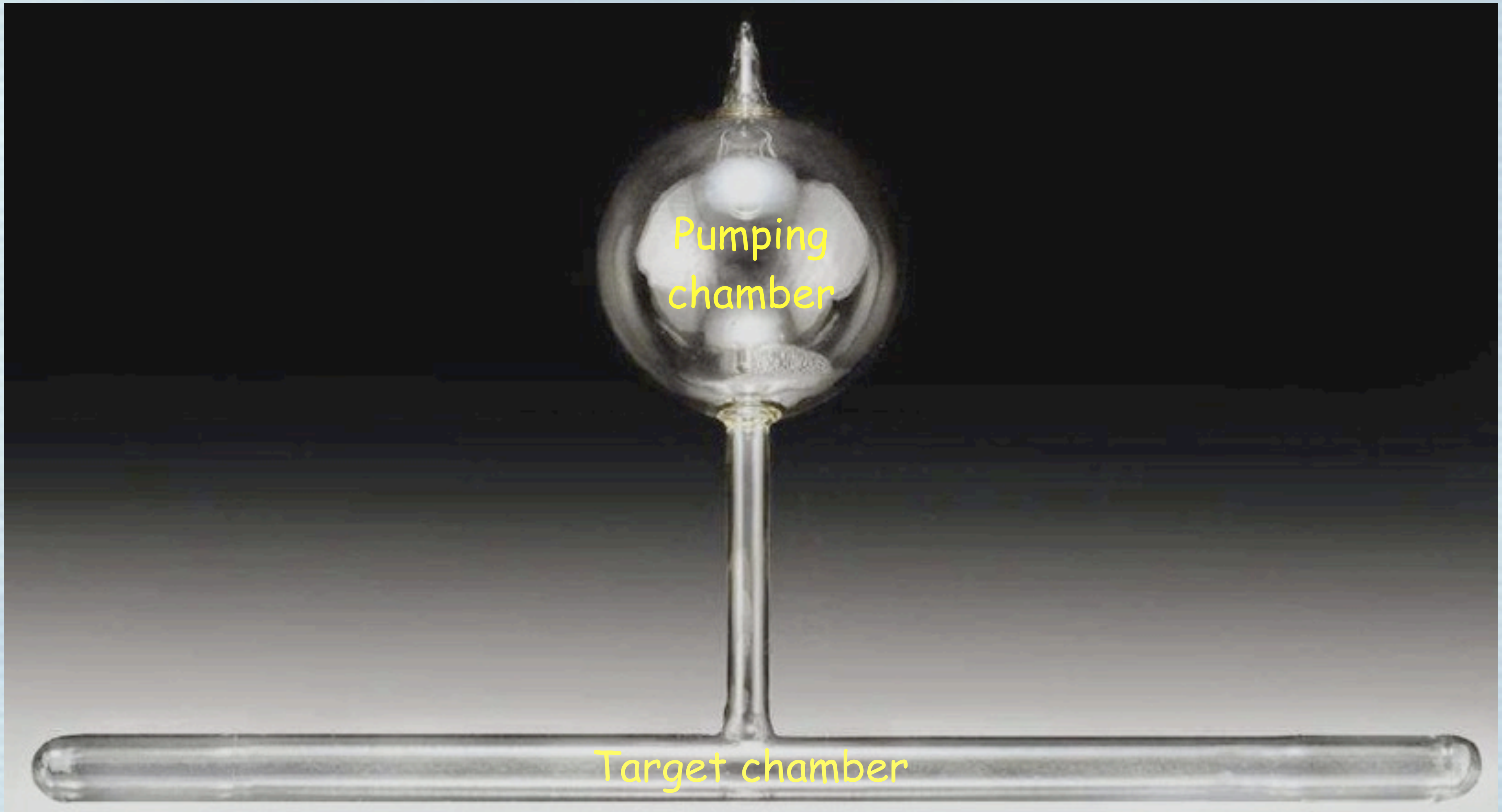

- Spin-exchange optical pumping in the upper “pumping chamber”
- Electron beam passes through the lower “target chamber”
- Polarized gas moves between the two chambers largely by convection.

One big step: Hybrid mixtures of Rb and K to greatly improve efficiency of spin transfer

- 1997 - ^{3}He-K spin relaxation predicted to be weaker than for ^{3}He-Rb: Walker, Thywissen and Happer, PRA vol. 56, pg 2090 (1997).
- 1998 - ^{3}He-K spin-exchange shown to be more efficient: Baranga et al. (incl. Romalis), PRL vol 80, 2801 (1998).
- 2001 - alkali-hybrid spin-exchange optical pumping suggested: Happer, Cates, Romalis, Erickson, U.S. Patent 6318092 (2001).
- 2003 - alkali-hybrid spin-exchange optical pumping demonstrated; Babcock, Nelson, Kadlecek, Driehuys, Anderson, Hersman and Walker, PRL vol 91, 123003 (2003)

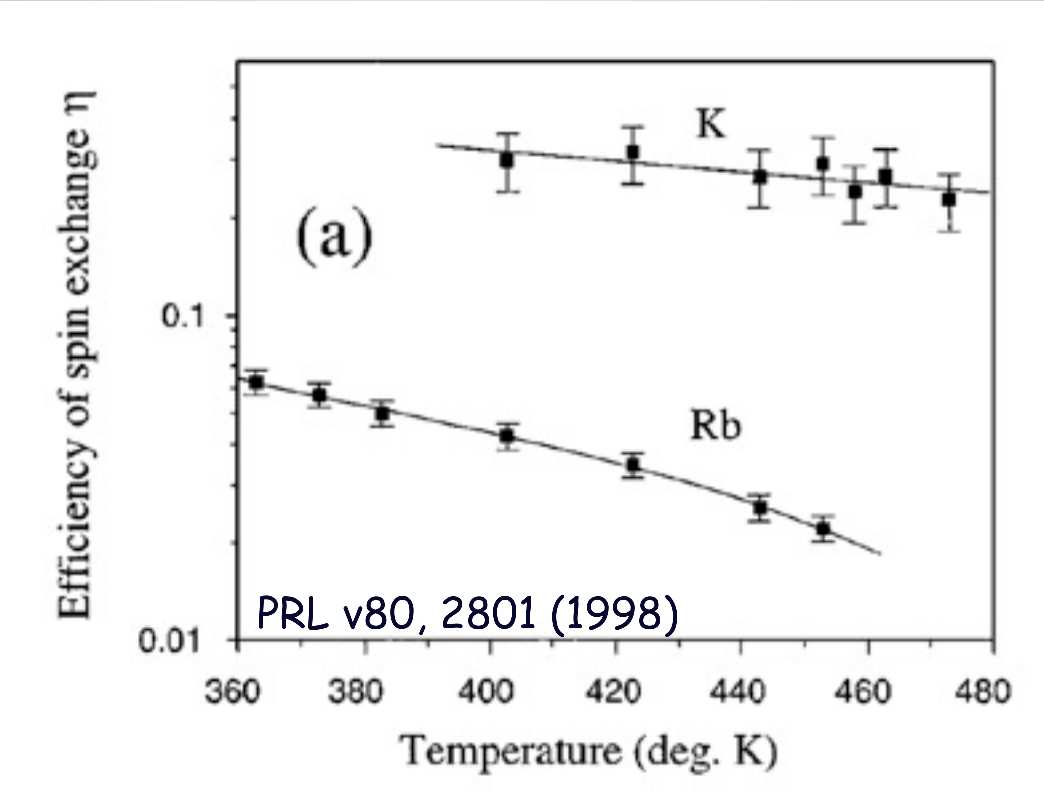

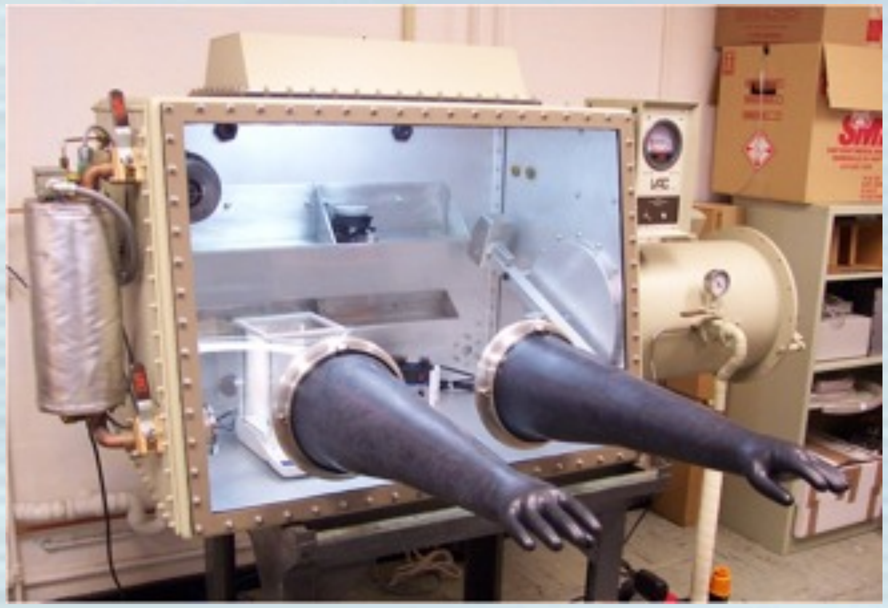

Alkali-hybrid SEOP polarized ^{3}He targets produce large gains, ~50% polarization, for E02-013, which measured GEn in Hall A

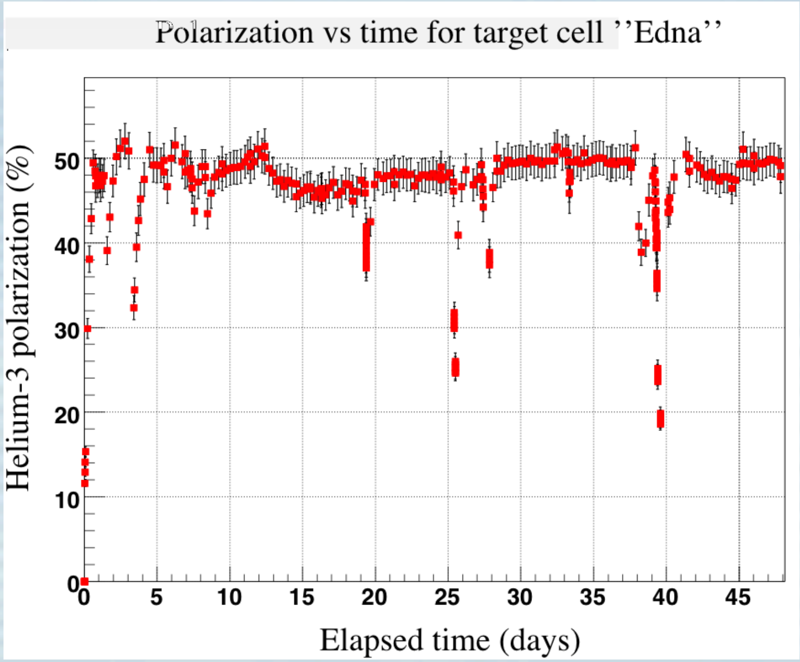

Selected experiments planned for the 12 GeV era

A_1^n in the 12 GeV era

projected errors and coverage

Hall A using BigBite

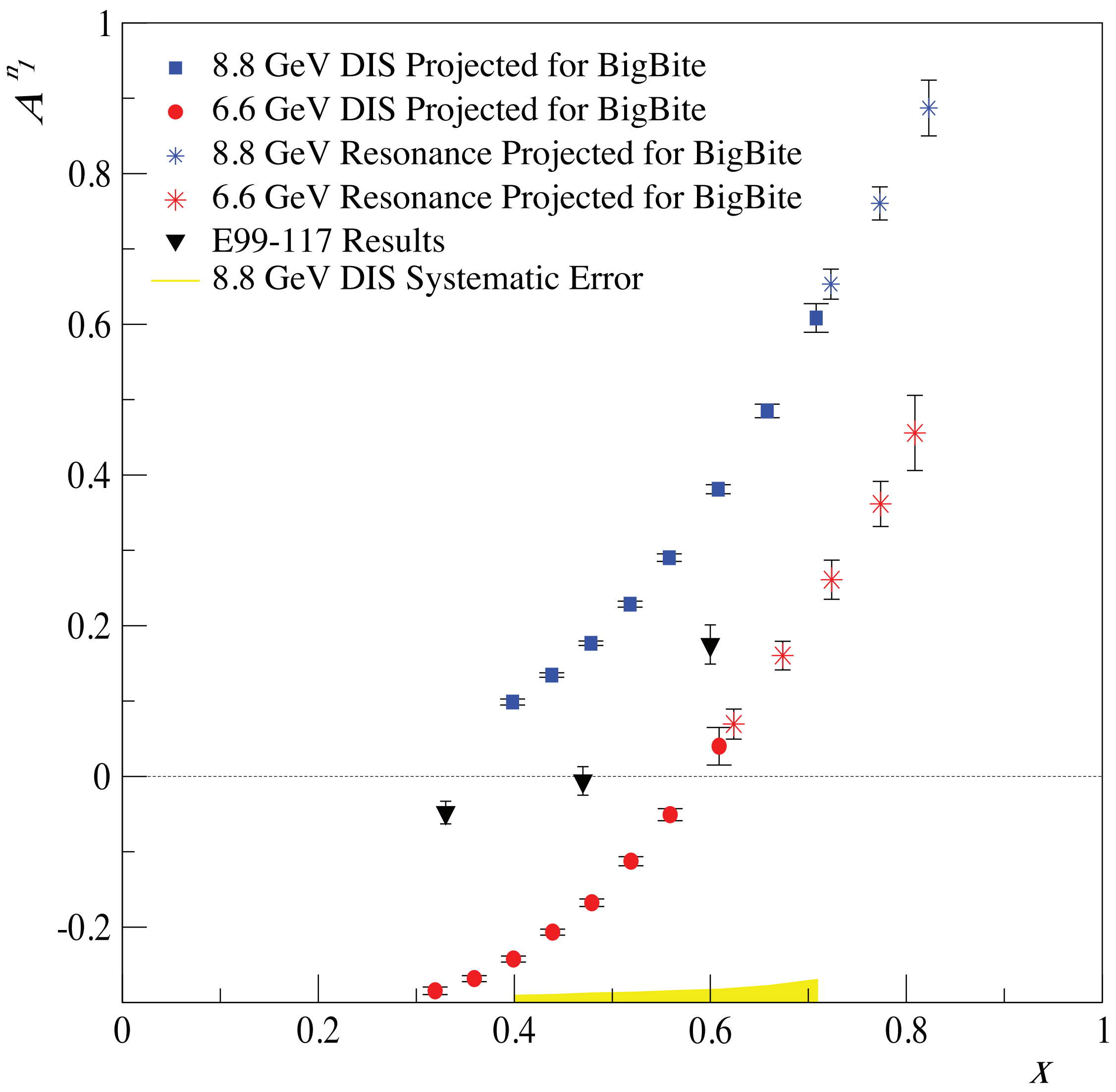

Hall C using SHMS and HMS

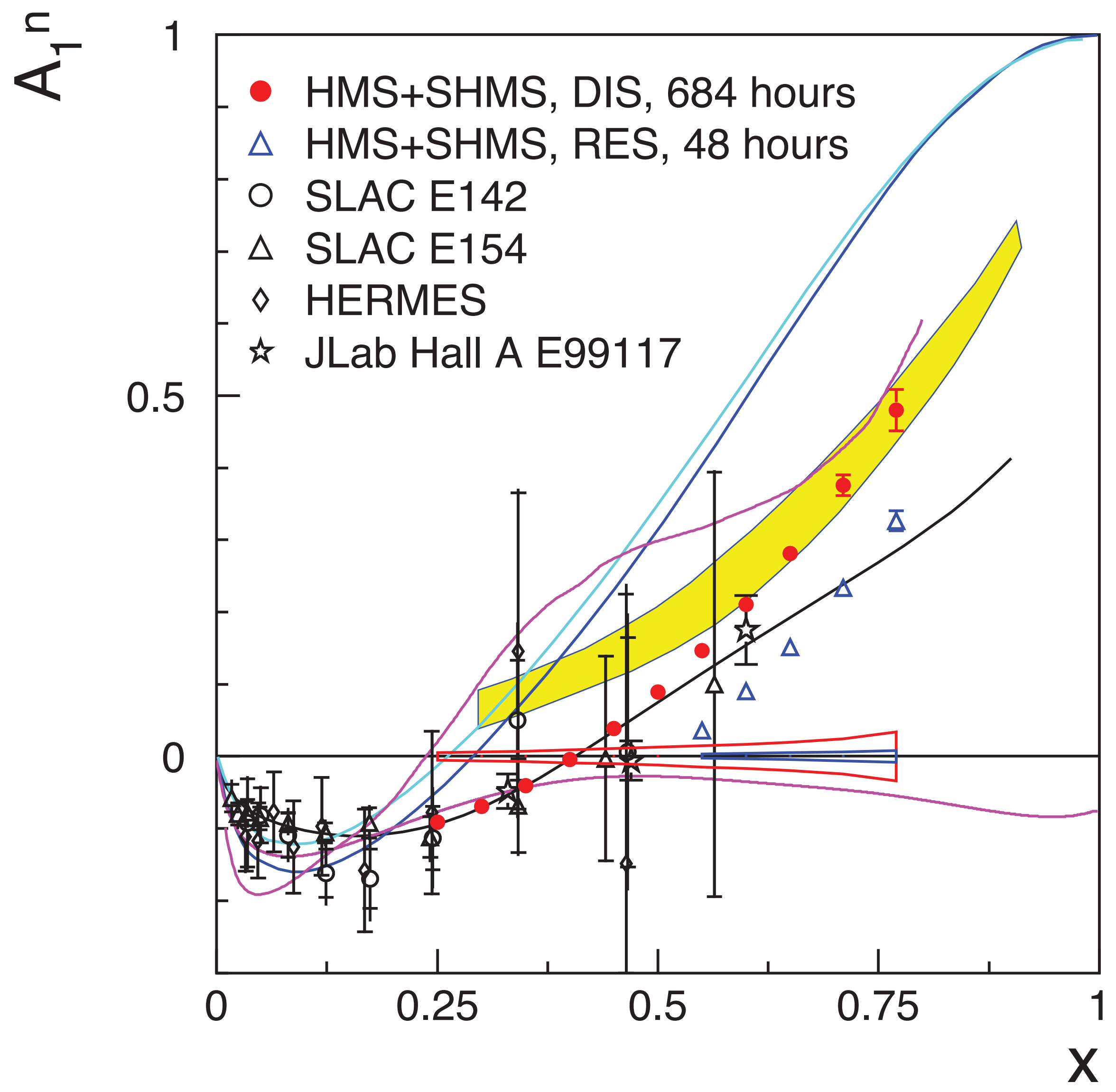

- Game-changing improvement in precision and coverage in x
- Major improvements in both the target and the spectrometer and detector systems.

Super Bigbite measurement of G_E^n/G_M^n

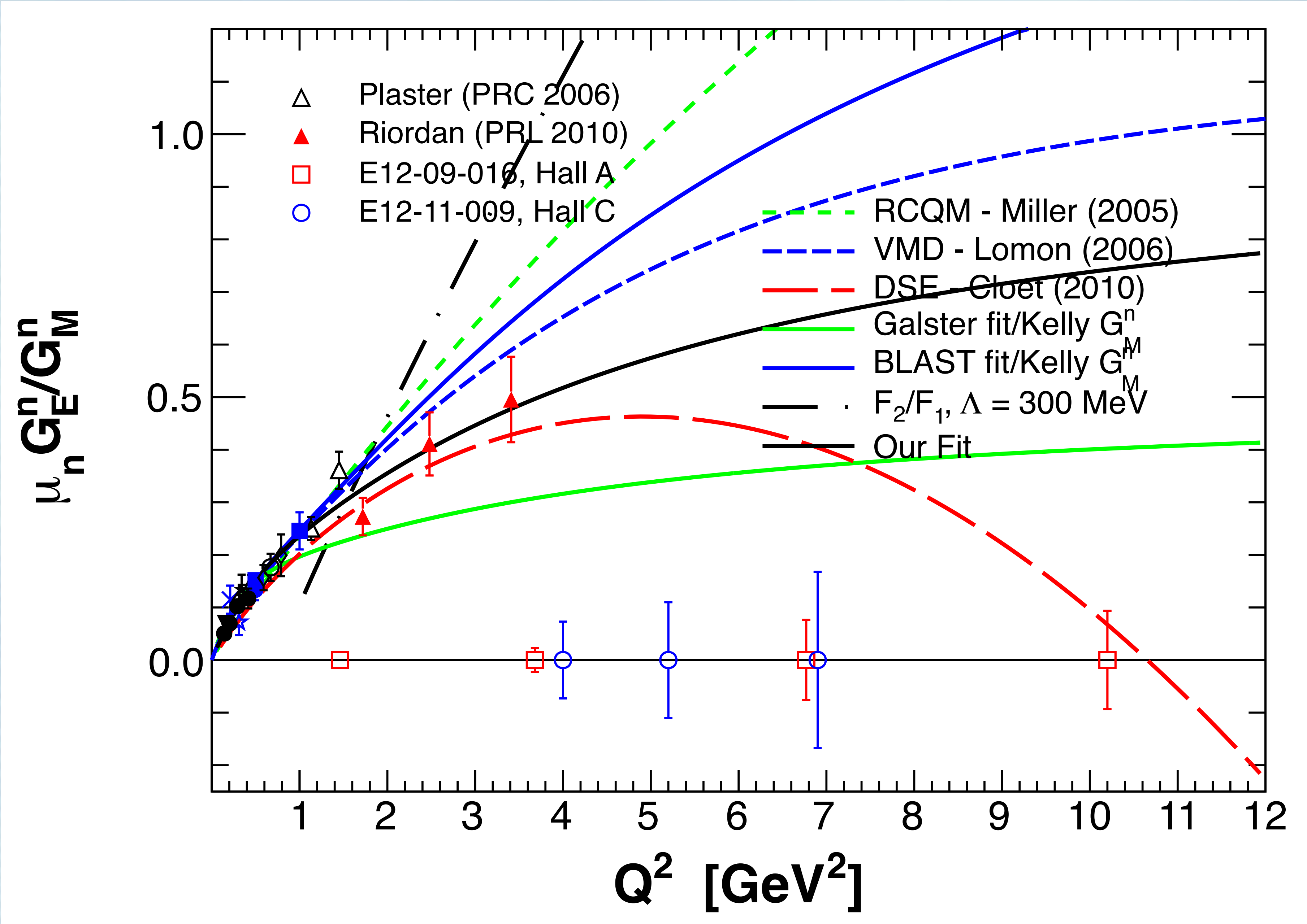

The three Super Bigbite experiments will meet the requirements to achieve the best physics by providing precise measurements at high Q^2.

Super Bigbite measurement of SSA in SIDIS using polarized ^{3}He

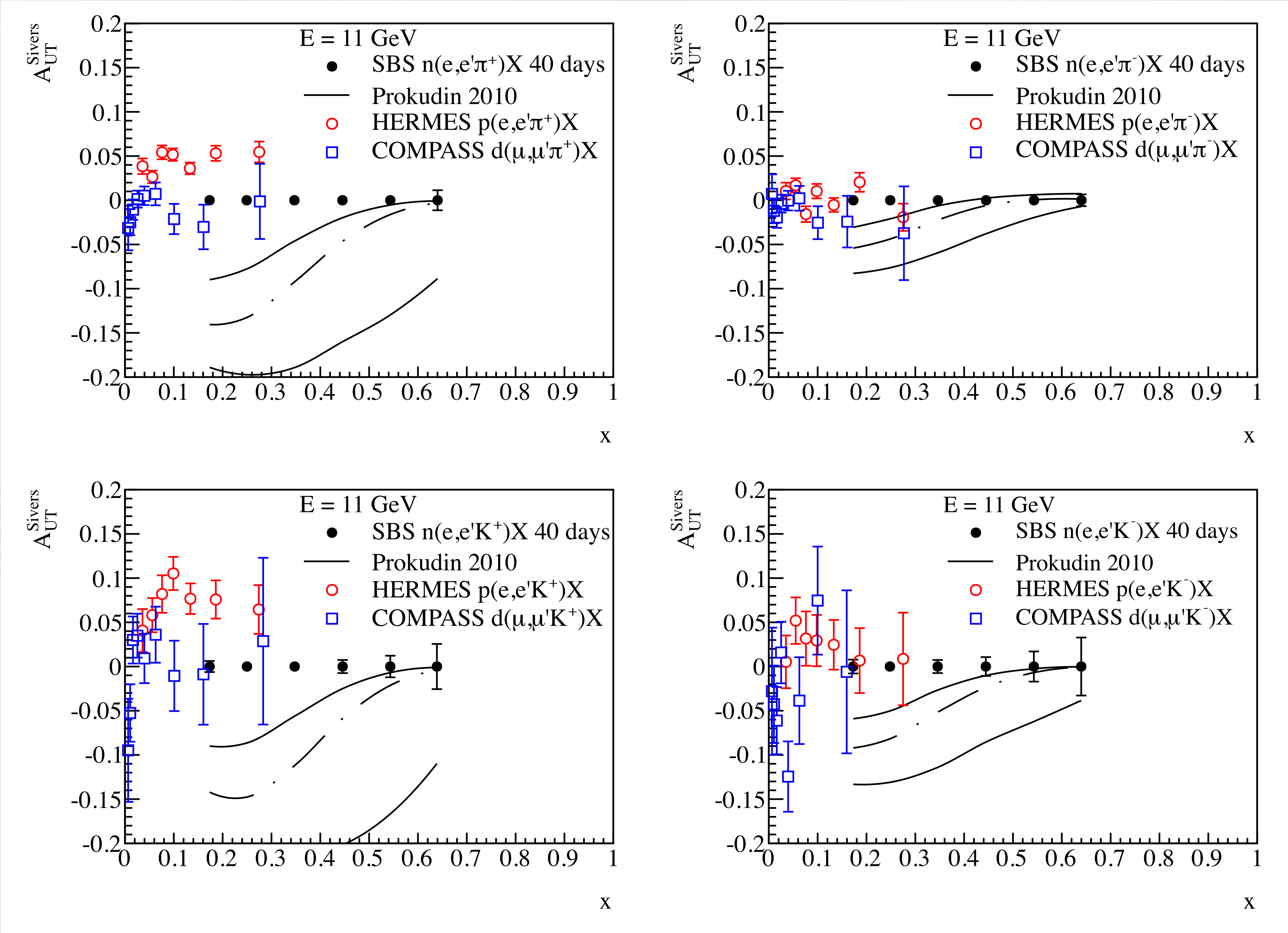

Roughly 100x statistical power of HERMES data

Polarized ^{3}He target requirements: past and future

Experiment	Current (μA)	Polarization	Luminosity	Effective Luminosity
SLAC E142	3.3	33%	1.5×10^{35}	1
GDH	12.5	35%	1.0×10^{36}	7.5
GEn	8	47%	6.1×10^{35}	8.2
Transversity	12	55%	9.0×10^{35}	16.7
Hall A A1n	30	65%	3.3×10^{36}	85.3
SBS GEn	60	62%	6.6×10^{36}	155.3
Hall C A1n	60	60%	6.6×10^{36}	145.5

Past

Future

Demonstrated through simulated beam tests

Important technology

- High-power diode-laser arrays (SLAC E154/JLab E-94-010 (GDH))
- Careful selection through full-power tests (E-99-117 (A1n))
- Alkali-hybrid spin-exchange optical pumping (GEn)
- Spectrally-narrowed high-power diode-laser arrays (Transversity)
- Convection-driven cells (demonstrated in bench tests)
- Metal end windows (in development)

Polarizaton gradients between the pumping and target chambers

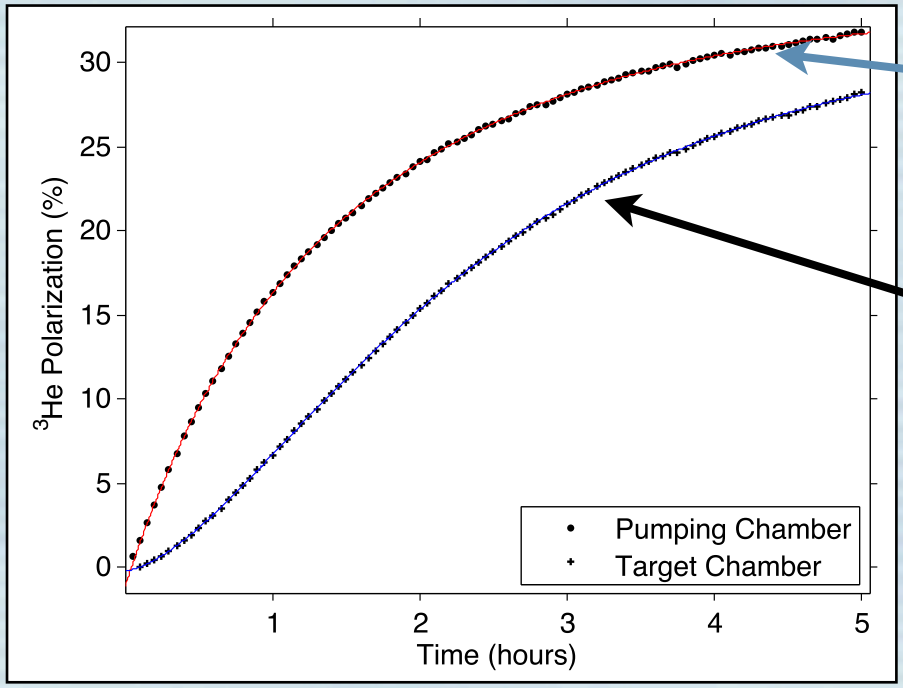

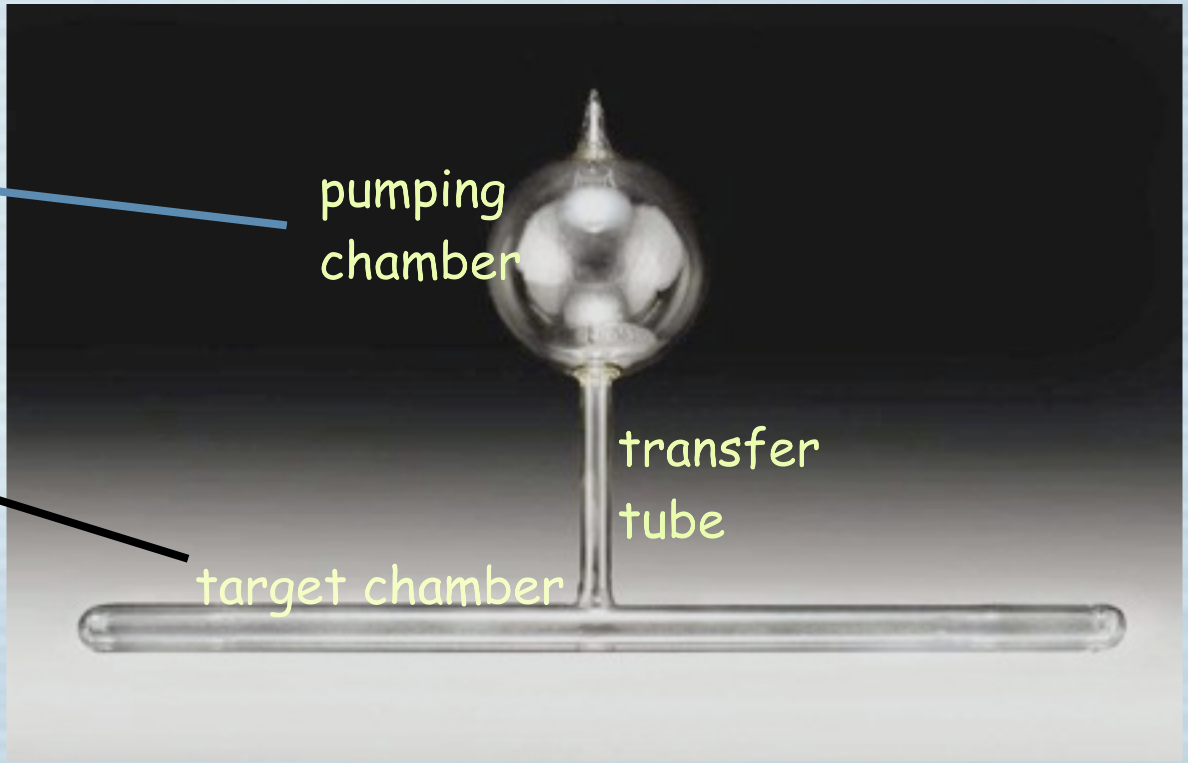

Diffusion limits mixing between the pumping and target chambers.
This problem would be crippling with the high-luminosity experiments planned for 12 GeV

Convection-based target cells

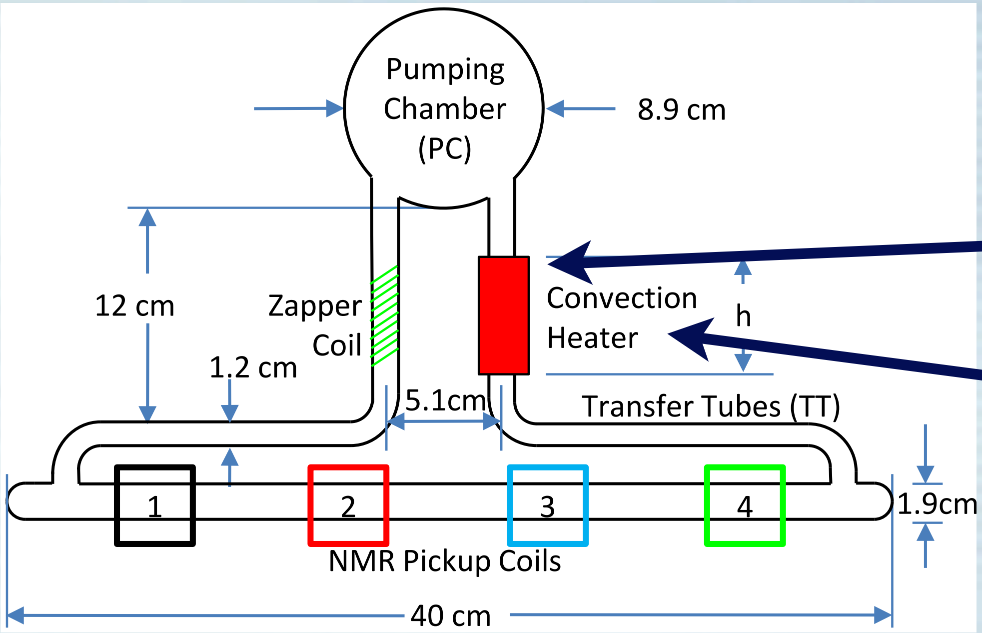

The convection-style cells have two transfer tubes instead of one.

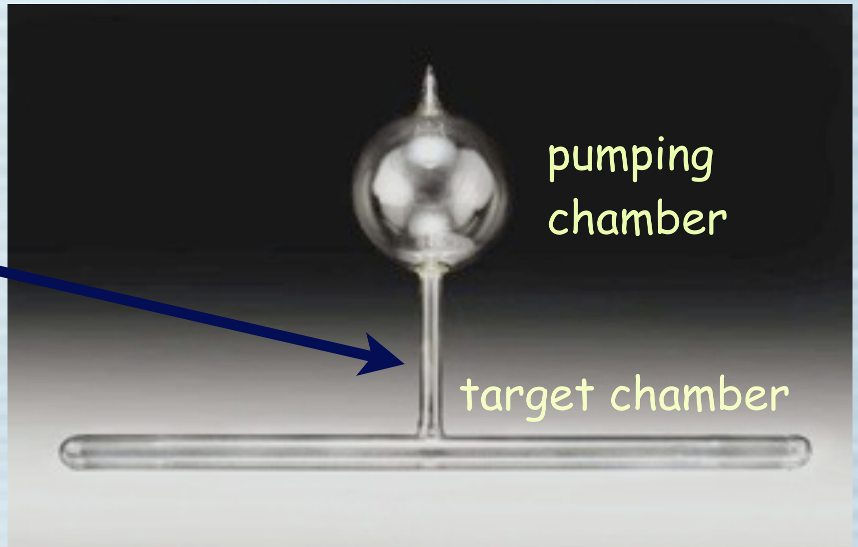

A small heater on one transfer tube creates a buoyancy force that induces convection

Measuring the gas speed

A "Zapper coil" is used to produce a depolarized slug of gas. Four NMR pickup coils register the passage of the slug of gas as a function of time.

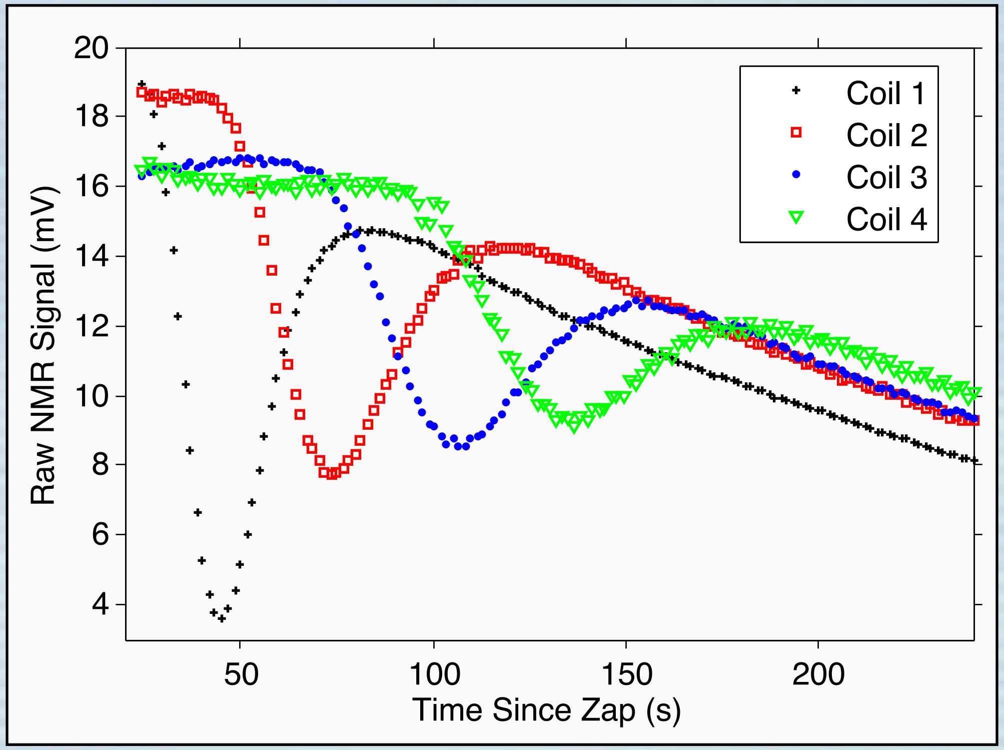

Dolph, Singh, Averett, Kelleher, Mooney, Nelyubin, Tobias Wojtsekhowski and Cates, PRC vol 84, pg 065201 (2011)

The first prototype quasi-next-generation polarized ^{3}He target

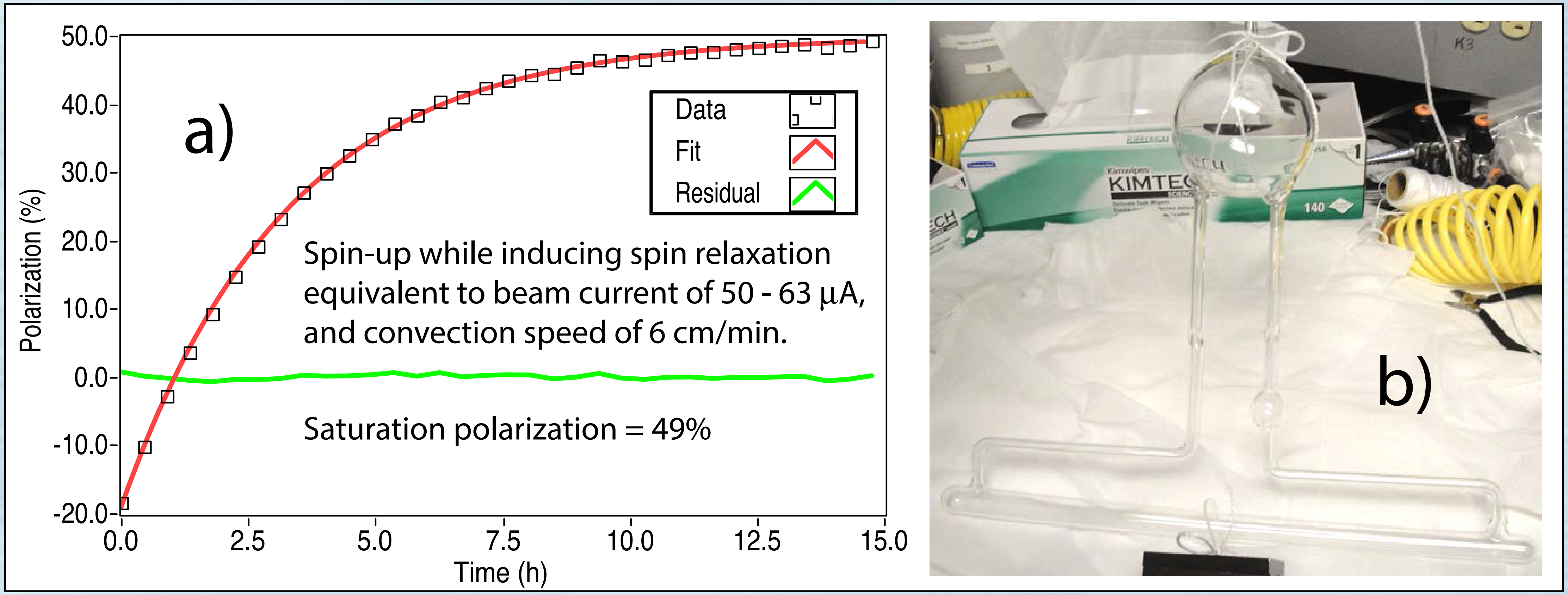

- Simulated beam test: P_{He} > 49% with 45 μA beam current.
- P_{He} ~ 67% with no convection (and no simulated beam).
- P_{He} ~ 61% with convection (and no simulated beam).
- P_{He} likely around 55-60%, with 30 μA beam current for actual target cell under full operating conditions.

For high beam currents, we would at least like metal end windows on the target chamber

We have had a long campaign trying to incorporate metal into cells successfully!

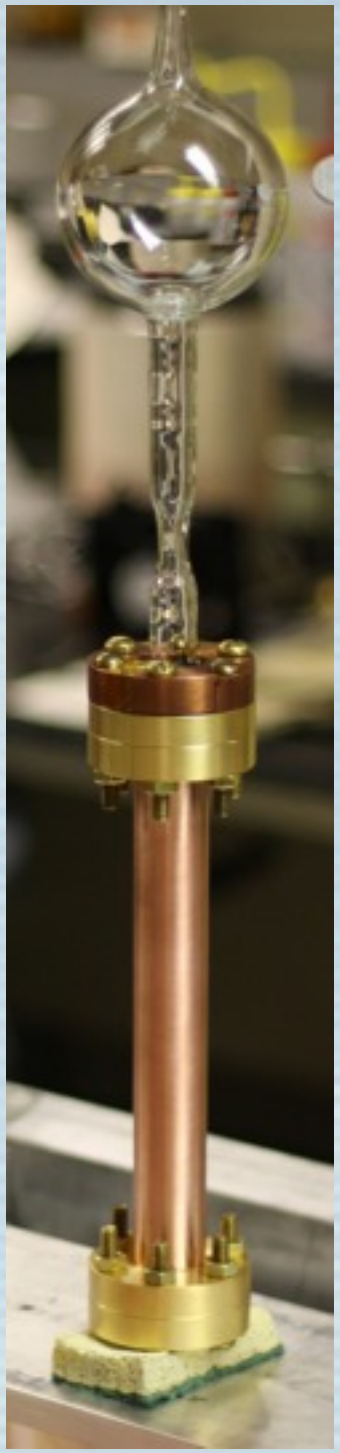

Technology (finally!) demonstrated for incorporating metal into our targets

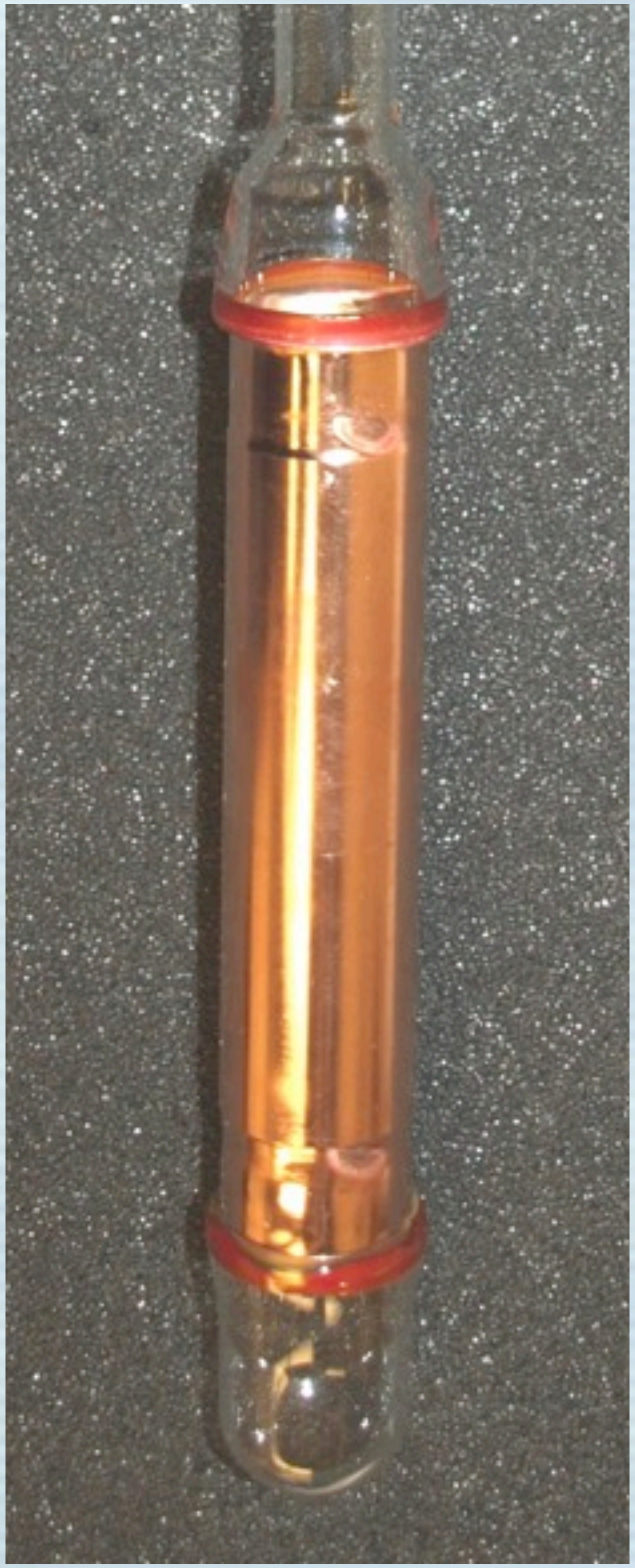

Several years of development working closely with Larson Glass (glass-to-metal seals), Epner Technology Inc. (electroplating) and Mike Souza (Princeton glass blower).

- OFHC Glass-to-metal seal provides excellent vaccuum/pressure integrity.
- Metal is first mechanically polished.
- Next the metal is electropolished.
- Gold is next electroplated onto the interior surface.
- Finally, the piece is incorporated into a cell.

“Spin-down” tests of cell GoldenVec II

GoldenVec-II

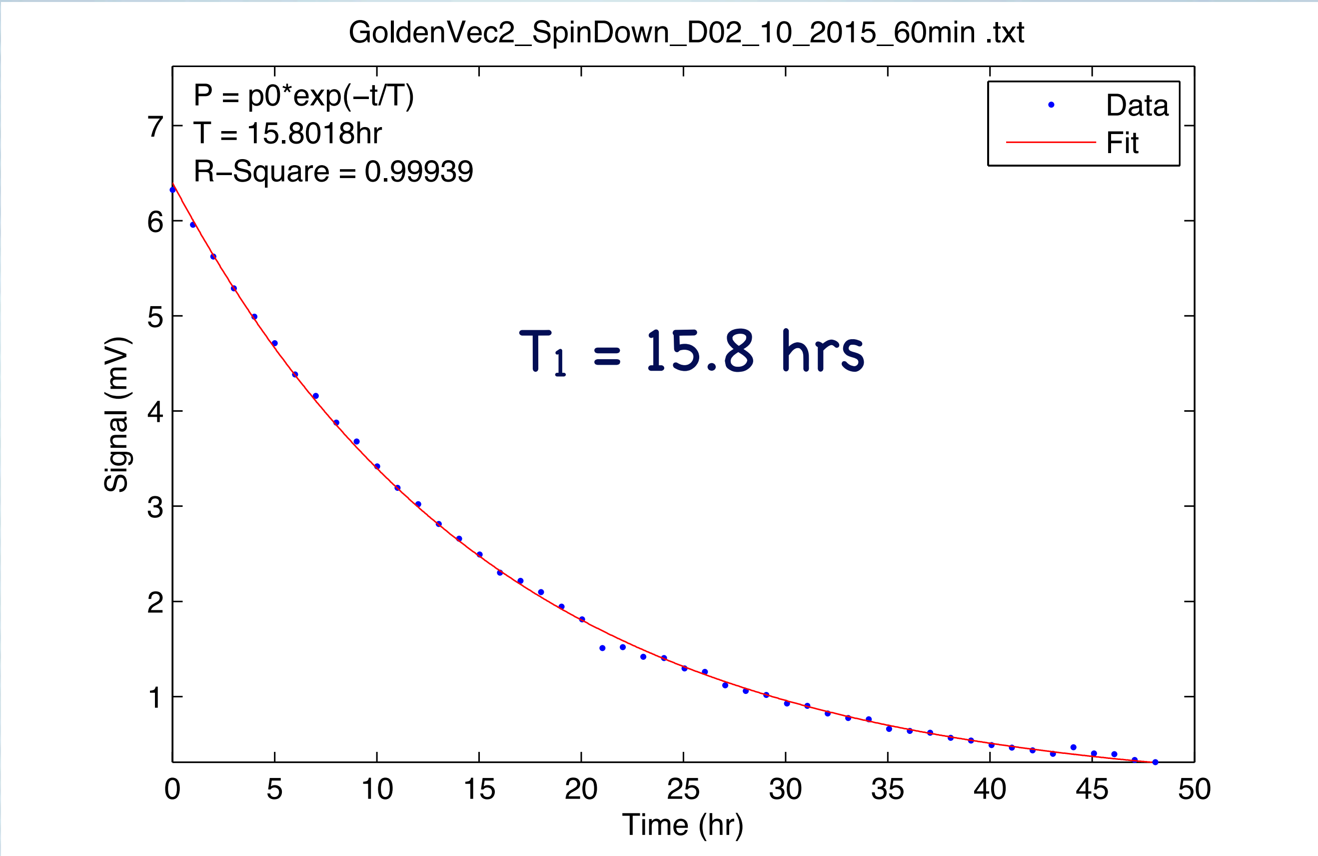

- This lifetime is not that different from some so-so target cells.
- MUCH less metal would be needed for metal end windows.
- This suggest negligible impact by adding metal end windows.
- We are now working toward incorporating this technology into a target cell.

Metal end windows

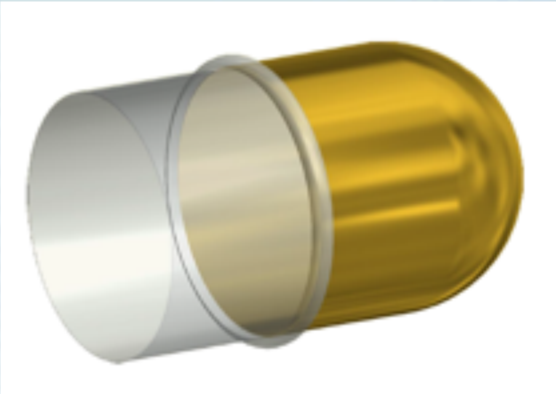

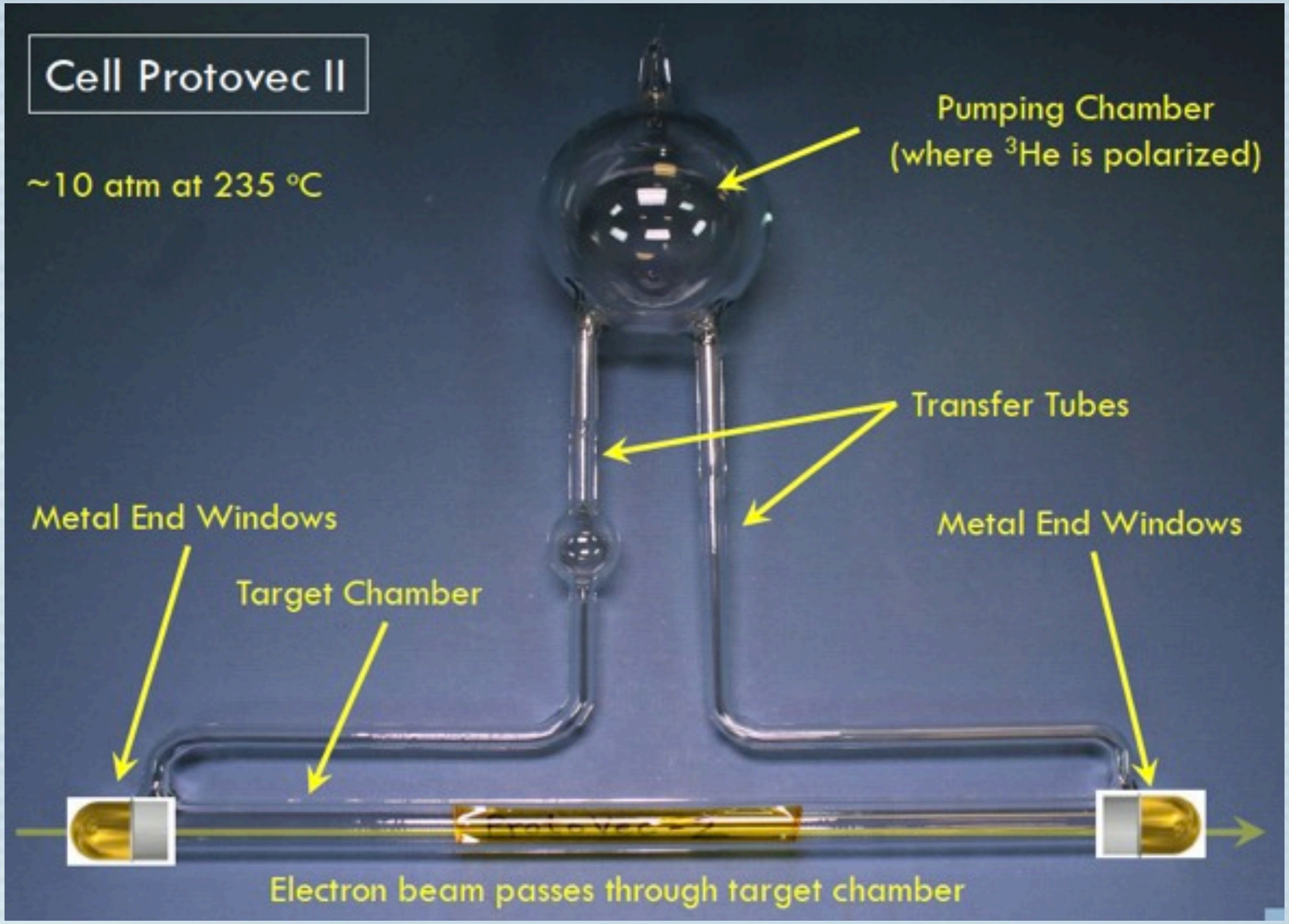

- Metal shape will be different, otherwise largely the same as in test cells.
- Gold-coated OFHC copper appears capable of achieving window thickness comparable to or smaller than glass windows.
- Gold-coated titanium may give us a factor of three or more.
- Am I being too conservative?

SBS Polarized ^{3}He target milestone #1: Selection of target cell design for G_E^n

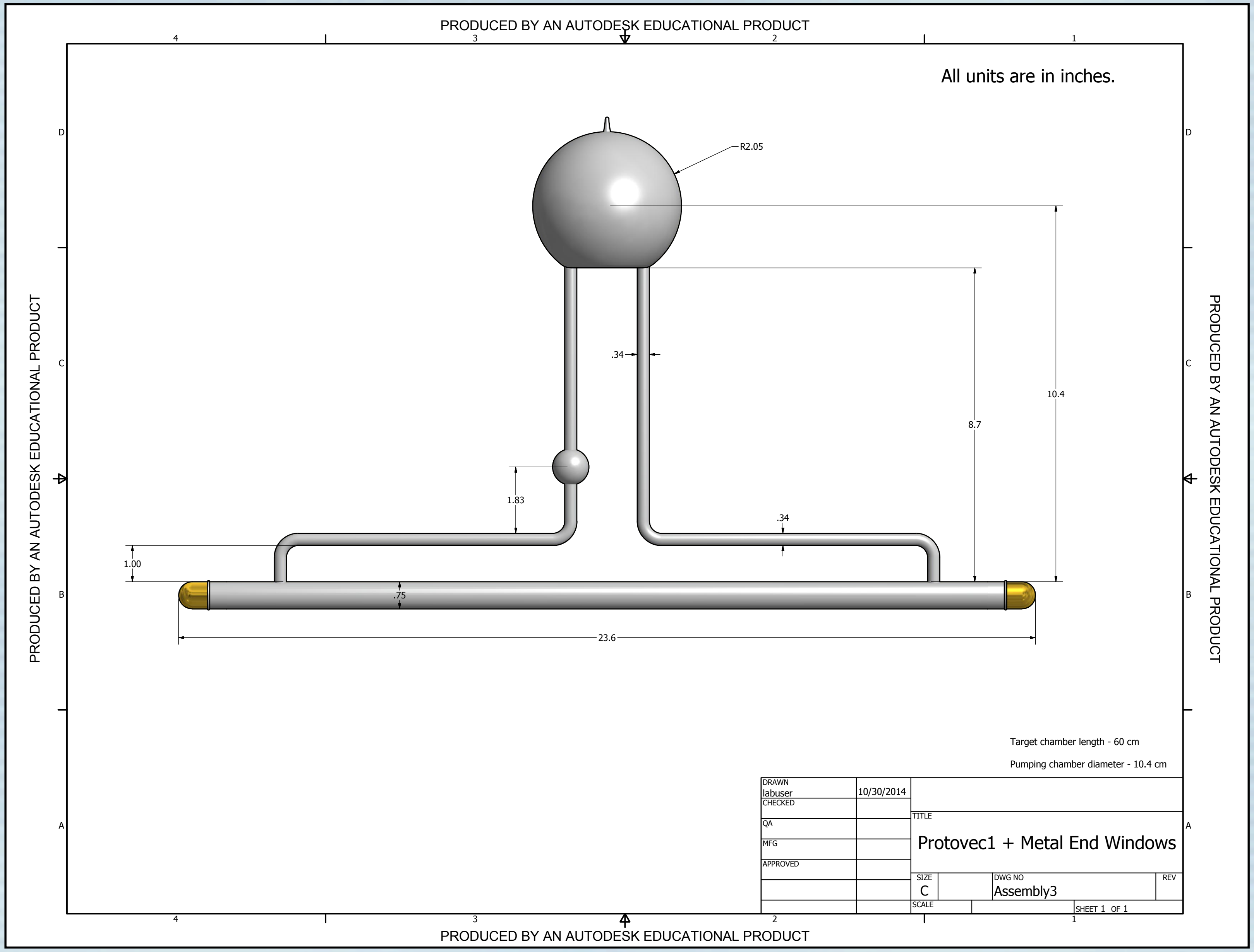

- Convection-based design, now well tested in Protovec-series cells.
- Contains 6 STP liters of ^{3}He in 750 cm^3 volume cell.
- OFHC copper metal end windows with gold electroplating on inner surface.
- 60 cm target-chamber length will deliver desired luminosity with 60 μA electron beam.

Issues specific to spectator tagging

- Presumably need VERY thin target walls.
- Glass could probably go down to a few hundred microns.
- Metal might be able to go further, if necessary, but this is harder.
- Issues are very different, in some ways better, for collider experiments.

Summary

- Many successful experiments behind us.
- 3rd generation polarized ^{3}He targets show greatly improved performance and are ready to exploit the JLab 12 GeV era.
- Targets for spectator tagging experiments could certainly be considered.

Jerry Miller's suggestion explaining the different scaling by using diquarks

u-quark scattering amplitude is dominated by scattering from the lone "outside" quark. Two constituents implies $1/Q^2$

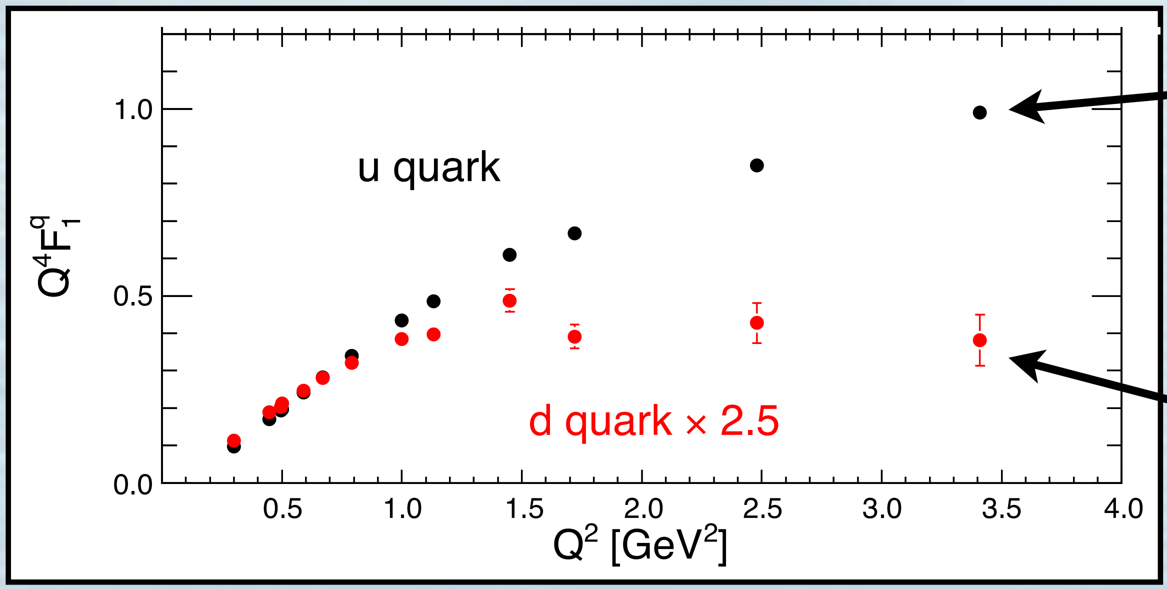

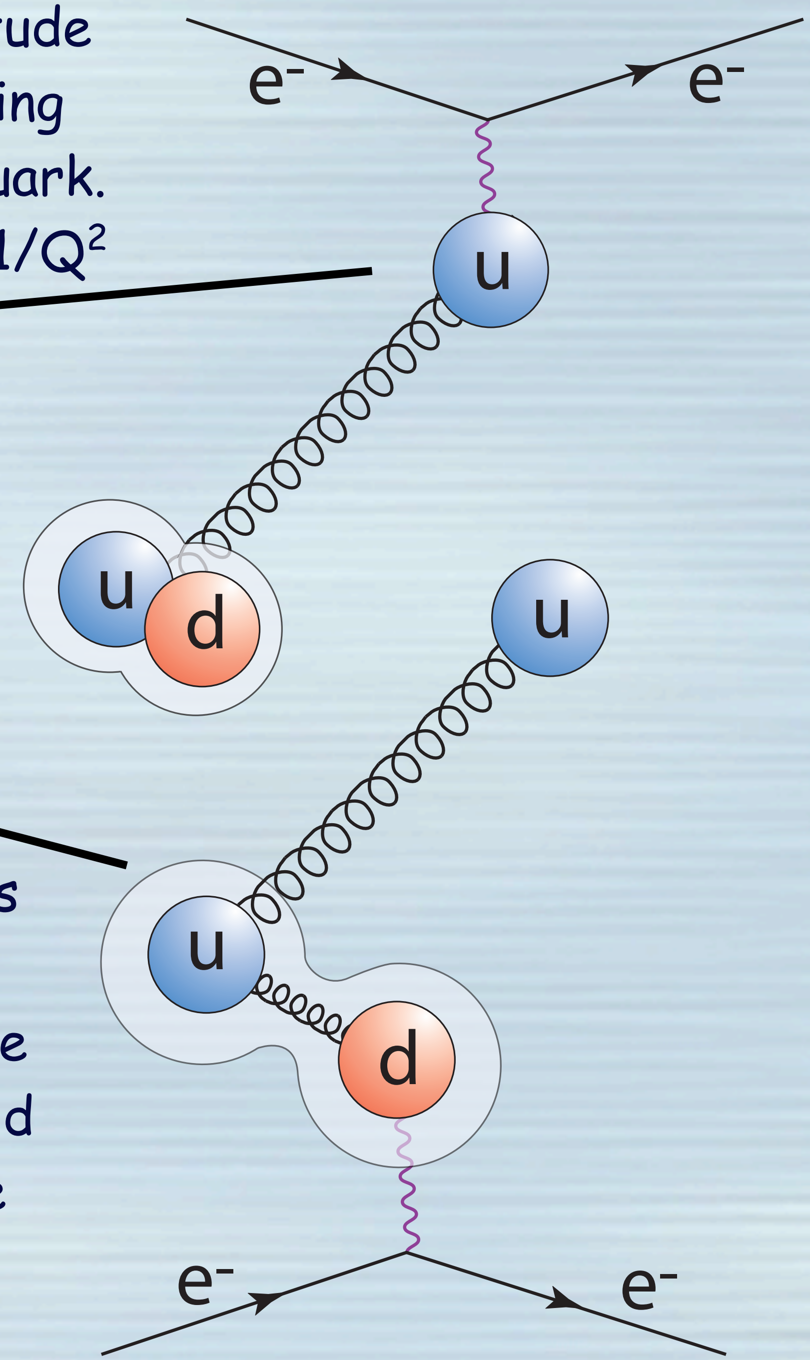

d-quark scattering amplitude is necessarily probing inside the diquark. Two gluons need to be exchanged (or the diquark would fall apart), so scaling goes like $1/Q^4$

While at present this idea is at the conceptual stage, it is an intriguingly simple interpretation for the very different behaviors.

Eliminating polarization graadients

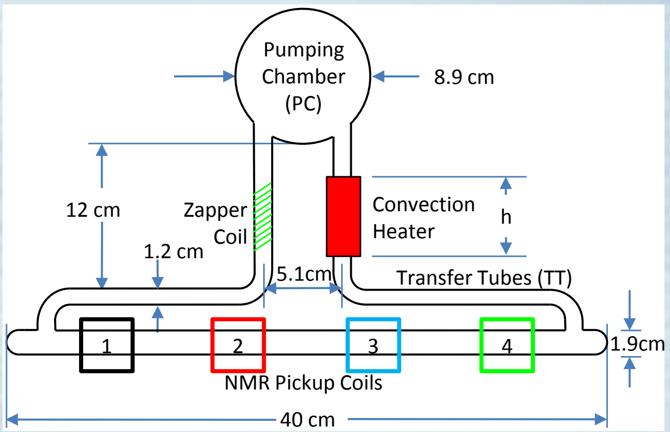

With convection-style cells, the velocity of the gas traveling through the target chamber can be easily controled from a few cm/min up to around 80 cm/min.

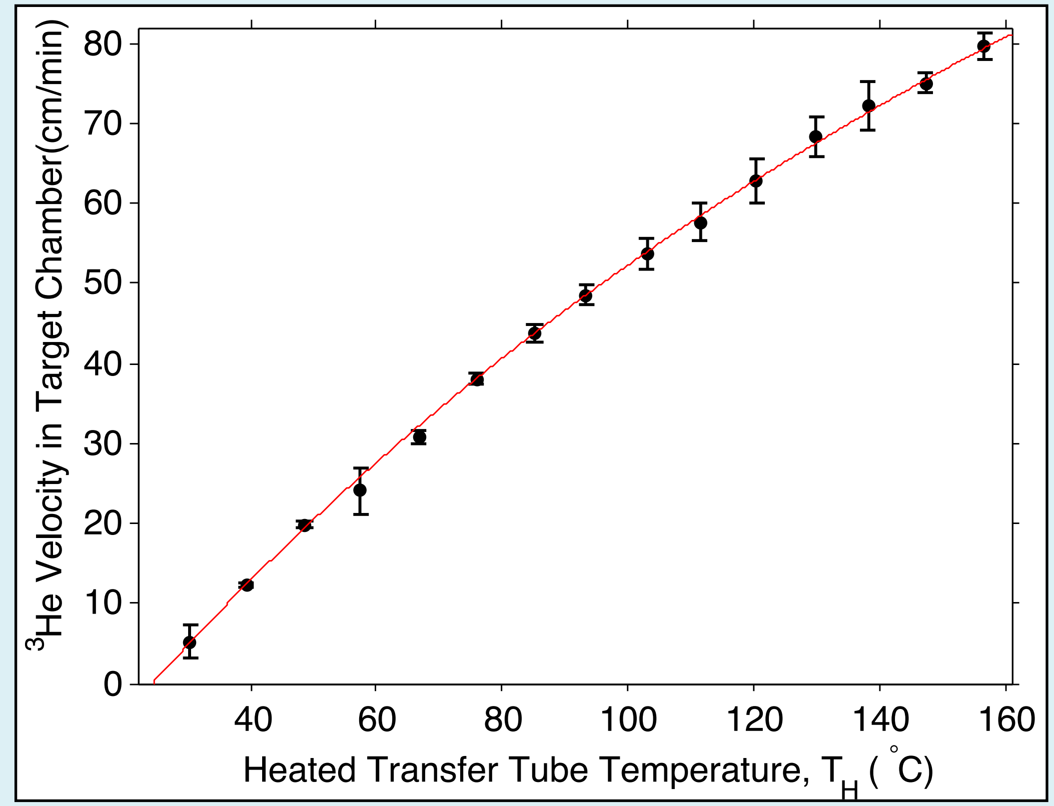

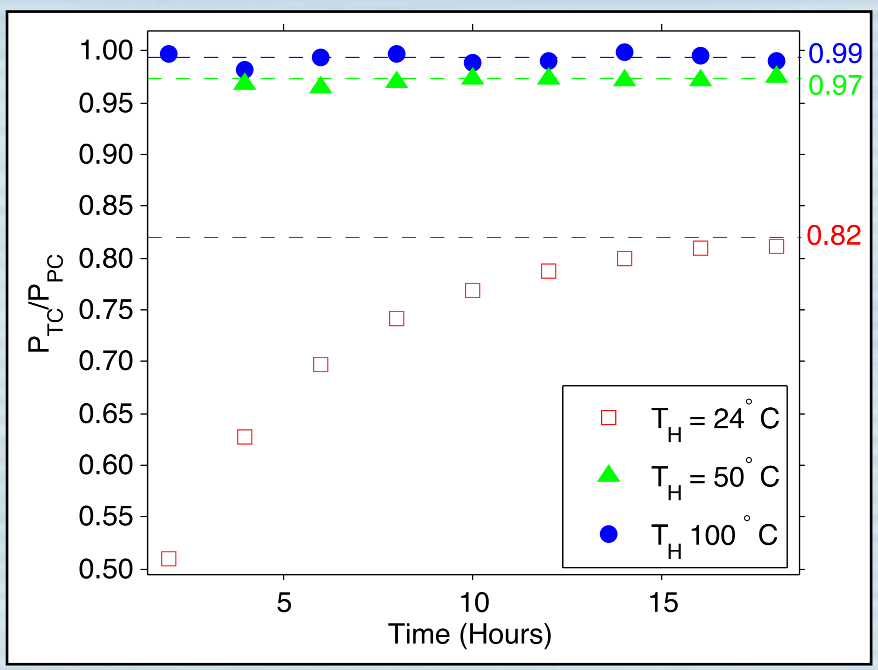

Polarization gradient: $$\frac{P^{\infty}_{\rm tc}}{P^{\infty}_{\rm pc}} = \frac{1}{1+\Gamma_{\rm tc}/d_{\rm tc}}$$

With V_{gas} = 6 cm/min,
$P_{tc}/P_{pc} > 0.98$ with beam, and
$P_{tc}/P_{pc} > 0.99$ with no beam.

With V_{gas} = 60 cm/min, $P_{tc}/P_{pc} > 0.999$!!!

Thus, convection also has implications for polarimetry

Protovec-style cells

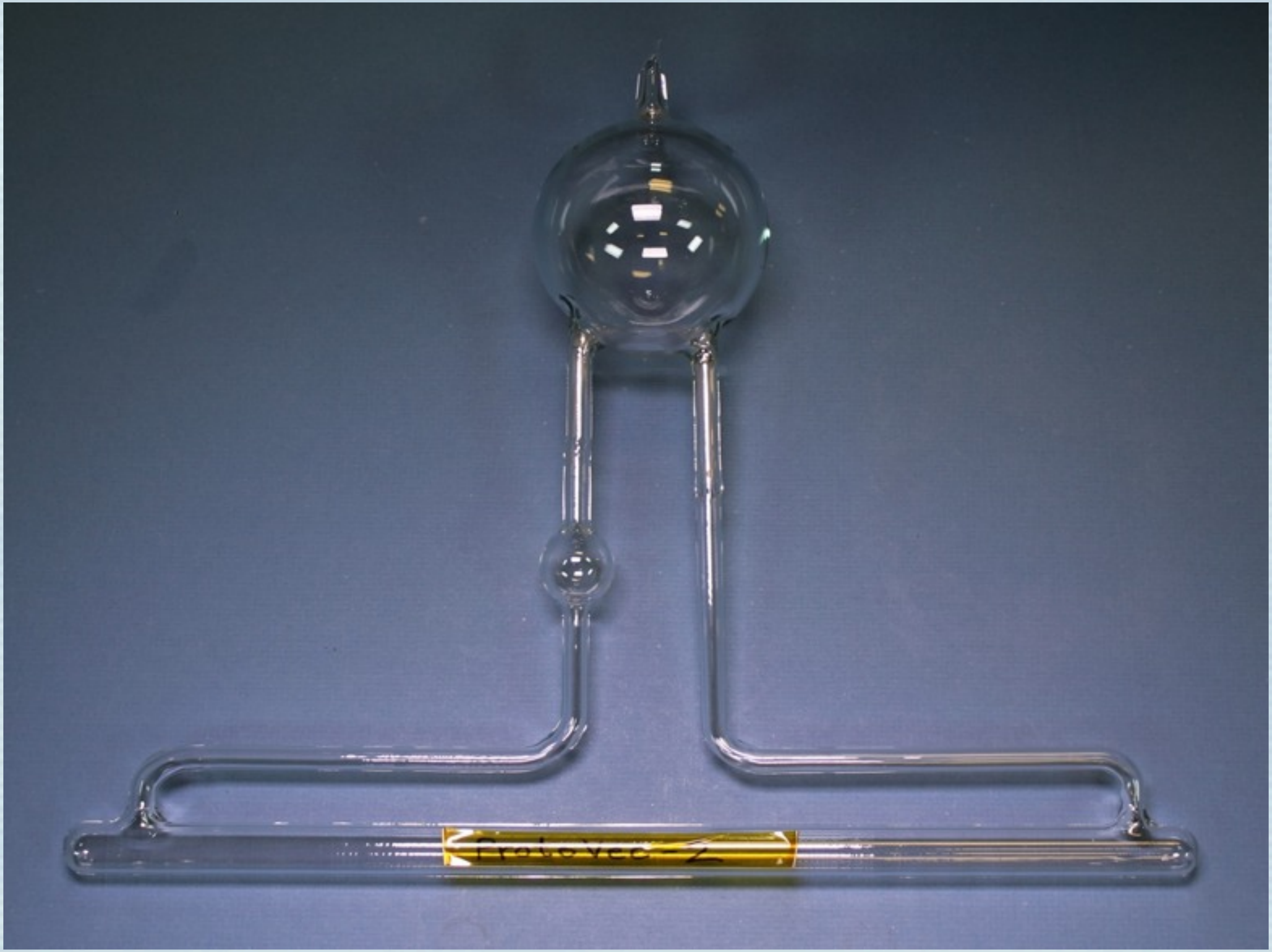

About to go into production

Why isn't P_{He} > 70%? -- The "X-factor"

The so-called X-factor characterizes a poorly understood temperature-dependent spin-relaxation mechanism that limits the maximum polarization of the target.

Babcock, Chann, Walker, Chen and Gentile
PRL vol. 96, pg. 083003 (2006)

$$\lim_{\gamma_{se}\to\infty} P_{\mathrm{He}} = \lim_{\gamma_{se}\to\infty} \frac{\langle P_{\mathrm{A}}\rangle\langle\gamma_{se}\rangle}{\langle\gamma_{se}\rangle(1+X)+\langle\Gamma_{\mathrm{He}}\rangle} = \frac{\langle P_{\mathrm{A}}\rangle}{1+X}$$

The new relaxation mechanism has been observed to be roughly proportional to the spin-exchange rate, so it cannot be overwhelmed by running the target "harder".

Indeed, the highest polarization reported in the PRL mentioned above is 79%, and there are VERY few examples in the literature claiming anything higher.

The X-factor

One way of measuring X-factors is by looking at spin-relaxation rates at different temperatures (and thus alkali densities).

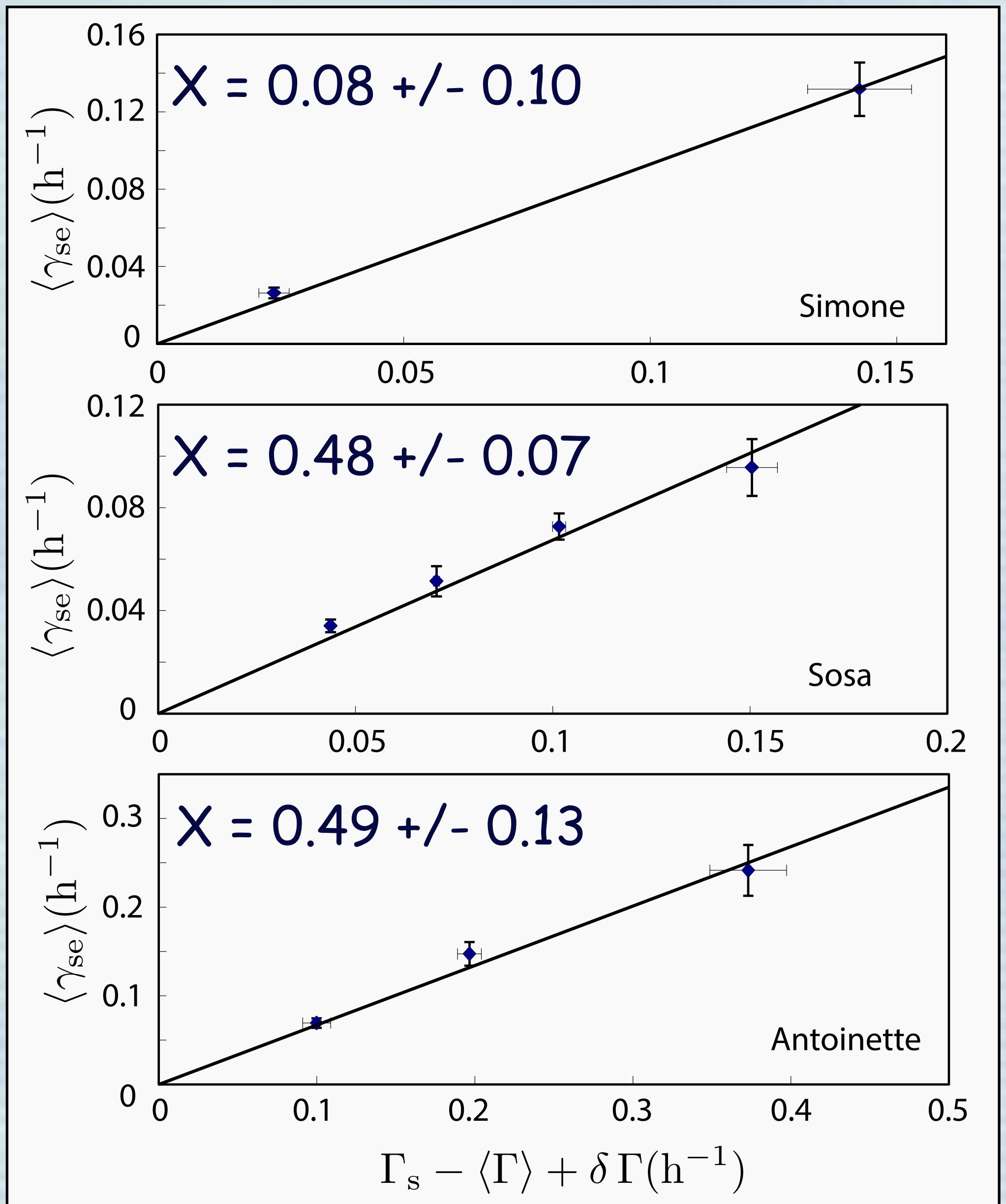

These quantities are determined by looking at "spin-ups" and cold "spin downs"

$$\langle\gamma_{se}\rangle = \frac{\Gamma_s - \langle\Gamma\rangle + \delta\Gamma}{(1+X)}$$

The <u>expected</u> spin-exchange rat is determined by measuring the alkali densities and using known spin-exchange coefficients

$$\gamma_{se} = k_{se}^{Rb}[Rb] + k_{se}^{K}[K]$$

The X-factor

X-factors can also be measured at a single temperature. We did so in a manner that overdetermined the X-factors, allowing both a better determination, as well as a check of internal consistency.

Cell	T(C)	X_1	X_2	X_3	X_4	X_{12}/X_{1234}
Sim.	215	-0.02(12)	-0.10(14)	-	-	-0.04(12)
	255	0.13(08)	0.08(09)	-	-	0.11(06)
Sosa	160	0.22(07)	0.28(09)	0.32(15)	0.18(09)	$0.24(06)^{\dagger}$
	170	0.24(07)	0.37(15)	-	-	0.27(06)
	180	0.45(08)	0.40(09)	0.50(17)	0.45(09)	$0.43(06)^{\dagger}$
	190	0.59(16)	0.57(17)	-	-	0.58(12)
Boris	235	0.21(14)	0.31(14)	-	-	0.26(10)
Sam.	235	0.08(06)	0.22(09)	-	-	0.12(05)
Alex	235	0.34(09)	0.35(09)	0.63(20)	0.29(10)	$0.34(06)^{\dagger}$
Astral	235	0.15(07)	0.22(10)	0.20(14)	0.14(07)	$0.17(05)^{\dagger}$
Steph.	235	0.31(17)	0.31(10)	-	-	0.31(08)
Brady	235	0.13(07)	0.15(09)	0.23(14)	0.11(07)	$0.14(05)^{\dagger}$
Antoinette	215	0.27(09)	0.44(17)	0.30(19)	0.25(11)	$0.28(08)^{\dagger}$
	235	0.20(09)	0.34(12)	0.36(17)	0.15(09)	$0.24(07)^{\dagger}$
	255	0.55(26)	0.54(16)	0.50(30)	0.56(26)	$0.55(13)^{\dagger}$

The X-factor

We see evidence suggesting there may be temperature dependence in the X-factor, a possibility explicitly mentioned by Babcock et al.

Cell	T(C)	X_1	X_2	X_3	X_4	X_{12}/X_{1234}
Sim.	215	-0.02(12)	-0.10(14)	-	-	-0.04(12)
	255	0.13(08)	0.08(09)	-	-	0.11(06)
Sosa	160	0.22(07)	0.28(09)	0.32(15)	0.18(09)	0.24(06)†
	170	0.24(07)	0.37(15)	-	-	0.27(06)
	180	0.45(08)	0.40(09)	0.50(17)	0.45(09)	0.43(06)†
	190	0.59(16)	0.57(17)	-	-	0.58(12)
Boris	235	0.21(14)	0.31(14)	-	-	0.26(10)
Sam.	235	0.08(06)	0.22(09)	-	-	0.12(05)
Alex	235	0.34(09)	0.35(09)	0.63(20)	0.29(10)	0.34(06)†
Astral	235	0.15(07)	0.22(10)	0.20(14)	0.14(07)	0.17(05)†
Steph.	235	0.31(17)	0.31(10)	-	-	0.31(08)
Brady	235	0.13(07)	0.15(09)	0.23(14)	0.11(07)	0.14(05)†
Antoinette	215	0.27(09)	0.44(17)	0.30(19)	0.25(11)	0.28(08)†
	235	0.20(09)	0.34(12)	0.36(17)	0.15(09)	0.24(07)†
	255	0.55(26)	0.54(16)	0.50(30)	0.56(26)	0.55(13)†

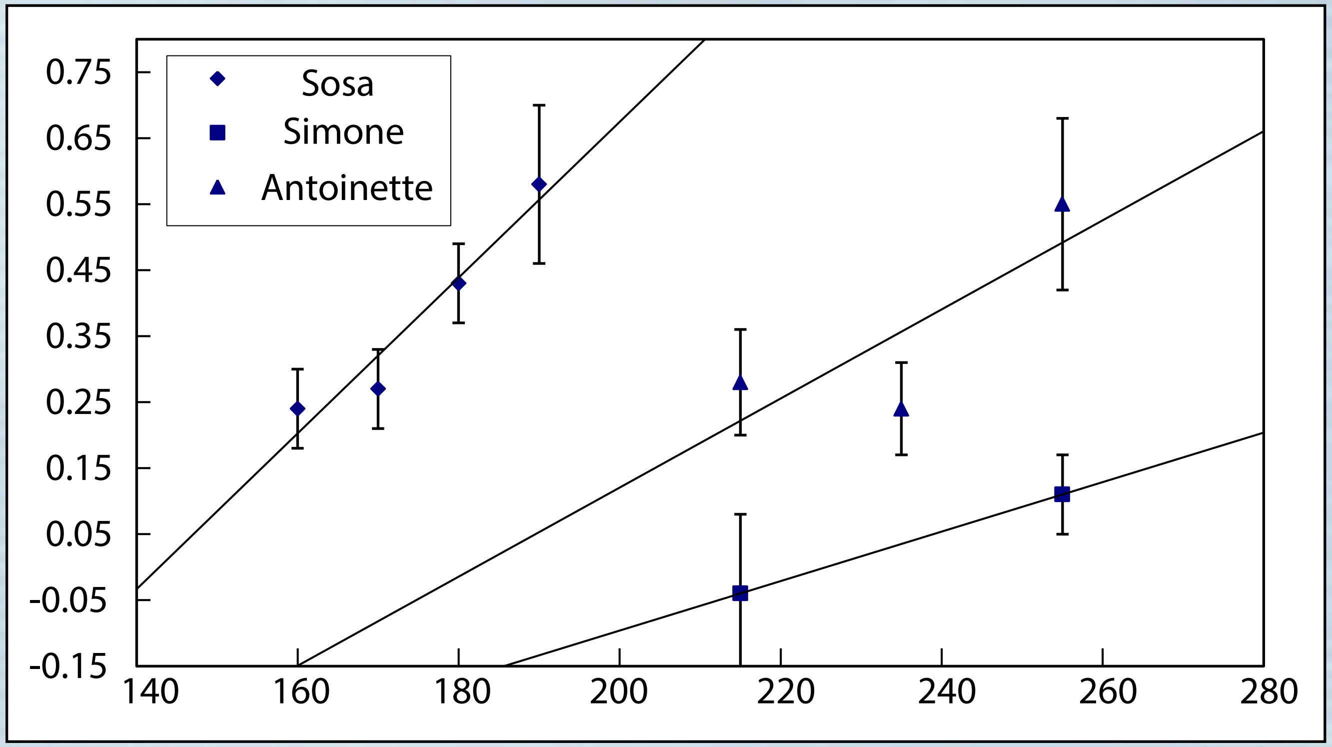

If true, X factors may represent an even more limiting ceiling on the polarization of SEOP ^3He targets

EXP	Cell	Lasers	I_0 W/cm^2	T_{pc}^{set} °C	P_{pc}^{∞}	Γ_s^{-1} hrs	$\langle\Gamma\rangle^{-1}$ hrs	$\frac{\langle P^A \rangle}{P^A_{line}}$	P^A_{line}	D_{fr}	D_{pb}	$[Rb]_{fr}$ 10^{14}/cm^3	ΔT_{Rb} °C	ΔT_{He} °C	X
saGDH	Proteus	3B	3.8	180	0.46	27	74	-	-	0	0	-	-	-	-
	Priapus	3B	3.8	180	0.44	21	56	-	-	0	0	-	-	-	-
	Penelope	3B	3.8	180	0.39	18	46	-	-	0	0	-	-	-	-
	Powell	3B	3.8	180	0.38	13	25	-	-	0	0	-	-	-	-
	Prasch	3B	3.8	180	0.33	13	33	-	-	0	0	-	-	-	-
GEN	Al	2.5B	3.2	235	0.53(03)	7.86(05)	27.42(1.37)	-	-	-	4.53(25)	-	-	-	-
		5B	6.1	235	0.54(03)	6.73(18)	27.42(1.37)	-	-	-	4.53(25)	-	-	-	-
	Barbara	2.5B	1.6	235	0.37(02)	5.50(08)	42.95(2.15)	-	-	-	4.80(25)	-	-	-	-
		5B	3.1	235	0.57(03)	4.76(63)	42.95(2.15)	-	-	-	4.80(25)	-	-	-	-
	Gloria	3B	1.7	235	0.60(03)	6.13(04)	38.29(1.91)	-	-	-	7.20(40)	-	-	-	-
	Anna	1B	0.6	235	0.33(02)	5.60(34)	11.38(57)	-	-	-	9.64(57)	-	-	-	-
		1.5B	1.0	235	0.39(02)	5.37(08)	11.38(57)	-	-	-	9.64(57)	-	-	-	-
	Dexter	1.5B	1.5	235	0.47(02)	7.58(17)	18.45(92)	-	-	-	-	-	-	-	-
		5B	6.1	235	0.49(02)	6.63(12)	18.45(92)	-	-	-	-	-	-	-	-
	Edna	3B	2.4	235	0.56(03)	5.71(02)	27.42(1.37)	-	-	-	3.63(20)	-	-	-	-
	Dolly	3B	1.0	235	0.43(02)	6.16(03)	35.24(1.76)	-	-	-	20(1.3)	-	-	-	-
		1N1B	1.4	235	0.62(03)	5.79(07)	35.24(1.76)	-	-	-	20(1.3)	-	-	17(10)	-
	Simone	2N1B	3.8	215	0.31(01)	14.08(06)	22.87(1.14)	0.947(020)	0.91(05)	10.66(54)	8.89(45)	0.20(02)	-7(3)	-	-0.04(12)*
		2N1B	3.8	240	0.48(02)	6.89(20)	22.87(1.14)	-	-	-	9.76(49)	-	-	-	-
		2N1B	3.8	255	0.58(02)	6.45(10)	22.87(1.14)	0.929(023)	0.92(05)	12.48(83)	10.3(52)	0.90(09)	-4(5)	-	0.11(06)*
	Sosa	2N1B	1.9	160	0.57(02)	16.69(09)	73.68(3.68)	0.966(020)	1.00(03)	0	0	1.97(13)	4(1)	30(7)	0.24(06)†
		2N1B	1.9	170	0.61(03)	11.67(04)	73.68(3.68)	0.964(020)	0.98(03)	0	0	3.00(33)	3(3)	38(14)	0.27(06)*
		2N1B	1.9	180	0.55(02)	8.79(09)	73.68(3.68)	0.954(022)	0.97(03)	0	0	4.30(27)	1(2)	47(7)	0.43(06)†
		2N1B	1.9	190	0.40(02)	6.39(22)	73.68(3.68)	0.854(075)	0.82(03)	0	0	5.69(63)	-2(3)	48(20)	0.58(12)*
		2N1B	1.9	200	0.26(01)	5.04(17)	73.68(3.68)	-	-	0	0	-	-	43(18)	-
Transversity	Boris	3B	1.8	235	0.42(02)	6.25(04)	23.74(1.19)	0.871(050)	0.79(07)	1.96(18)	2.45(23)	2.19(34)	-8(7)	-	0.26(10)*
	Samantha	3B	1.8	235	0.50(02)	6.30(13)	36.51(1.83)	-	-	-	4.34(23)	-	-	-	-
		3N	2.6	235	0.68(03)	4.62(03)	22.13(1.11)	0.956(020)	0.99(03)	4.37(10)	4.34(23)	1.80(10)	7(2)	21(10)	0.12(05)*
	Alex	2N1B	2.6	235	0.59(03)	4.81(02)	32.96(1.65)	0.942(042)	0.99(03)	1.37(08)	1.19(07)	4.08(36)	0(4)	42(10)	0.34(06)†
	Moss	1N1B	1.8	235	0.62(03)	5.35(04)	33.00(1.65)	-	0.95(09)	-	2.40(13)	-	-	29(8)	-
	Tigger	1N1B	1.8	235	0.51(02)	4.89(05)	12.62(63)	-	0.95(09)	-	-	-	-	23(9)	-
	Astral Weeks	2N1B	2.6	235	0.69(03)	6.57(12)	48.90(2.45)	0.954(020)	0.99(03)	7.09(55)	6.21(56)	0.97(09)	3(5)	25(4)	0.17(05)†
	Stephanie	3N	2.6	235	0.63(03)	4.55(09)	48.35(2.42)	0.929(114)	0.99(03)	1.39(11)	1.50(10)	5.08(58)	7(5)	54(6)	0.31(08)*
	Brady	1N	0.9	235	0.62(03)	4.82(1.08)	33.50(1.68)	-	0.95(03)	-	2.36(24)	-	-	14(9)	-
		2N	1.8	235	0.68(03)	5.52(70)	33.50(1.68)	-	0.99(03)	-	2.36(24)	-	-	25(8)	-
		3N	2.6	235	0.70(03)	5.30(01)	33.50(1.68)	0.956(021)	0.99(03)	2.60(20)	2.36(24)	2.86(30)	6(5)	39(9)	0.14(05)†
	Maureen	3N	2.6	235	0.66(03)	5.42(12)	29.21(1.46)	-	0.97(09)	-	4.42(55)	-	-	32(12)	-
	Antoinette	3N	1.7	215	0.49(02)	6.63(37)	20.93(1.05)	0.958(020)	0.99(03)	2.85(13)	-	0.96(07)	0(3)	16(8)	0.28(08)†
		3N	1.7	235	0.61(03)	4.18(10)	20.93(1.05)	0.936(043)	0.99(03)	3.32(27)	-	1.83(20)	0(5)	20(10)	0.24(07)†
		3N	1.7	255	0.41(02)	2.66(11)	20.93(1.05)	0.776(099)	0.93(10)	3.57(23)	-	2.88(39)	-5(6)	33(9)	0.55(13)†